



# Industria Textilă

ISSN 1222-5347 (97-144)

3/2010

Revistă cotate ISI și inclusă în Master Journal List a Institutului pentru Știința Informării din Philadelphia – S.U.A., începând cu vol. 58, nr. 1/2007/

ISI rated magazine, included in the ISI Master Journal List of the Institute of Science Information, Philadelphia, USA, starting with vol. 58, no. 1/2007

Editată în 6 nr./an, indexată și recenzată în:/

Edited in 6 issues per year, indexed and abstracted in:

Science Citation Index Expanded (SciSearch®), Materials Science Citation Index®, Journal Citation Reports/Science Edition, World Textile Abstracts, Chemical Abstracts, VINITI

## COLEGIUL DE REDACȚIE:

*Dr. ing. EMILIA VISILEANU*  
*cerc. șt. pr. I – EDITOR*

Institutul Național de Cercetare-Dezvoltare  
pentru Textile și Pielărie – București

*Prof. dr. ing. CRIȘAN POPESCU*

Institutul German de Cercetare a Lânii – Aachen

*Cerc. șt. pr. I ERIC BOUDON*

Institutul Francez de Textile-Îmbrăcăminte –  
Paris

*Prof. dr. ing. DUMITRU LIUȚE*  
Universitatea Tehnică Gh. Asachi – Iași

*Prof. dr. ing. AURELIA GRIGORIU*  
Universitatea Tehnică Gh. Asachi – Iași

*Prof. dr. ing. COSTEA BUDULAN*  
Universitatea Tehnică Gh. Asachi – Iași

*Prof. dr. ing. VALERIA GRIBINCEA*  
Universitatea Tehnică Gh. Asachi – Iași

*Ing. VASILE MIRCIU*

*director general adjunct*

Direcția Generală Politici Industriale –  
Ministerul Economiei și Comerțului

*Ing. VASILE PĂTRÂNIOIU – consilier*  
Ministerul Economiei și Comerțului

*Dr. ing. ION PIRNA – cerc. șt. pr. I*  
Institutul Național de Cercetare-Dezvoltare  
pentru Mașini Agricole – București

*Prof. dr. ing. EROL MURAD*

Universitatea Politehnică – București

*Dr. ing. MIHAELA IORDĂNESCU*  
*cerc. șt. pr. I – RENAR*

*Conf. dr. CRIȘAN ALBU*

Academia de Studii Economice – București

*Dr. ing. CARMEN GHITULEASA*  
*cerc. șt. pr. II*

Institutul Național de Cercetare-Dezvoltare  
pentru Textile și Pielărie – București

*Prof. ing. ARISTIDE DODU*  
*cerc. șt. pr. gr. I*

Membriu de onoare al Academiei  
de Științe Tehnice din România

*Ec. AURELIENȚIU POPESCU*  
*președinte executiv FEPAIUS*

*Prof. univ. dr. MARGARETA FLORESCU*  
Academia de Studii Economice – București

*Conf. univ. dr. ing.*

*LUCIAN CONSTANTIN HANGANU*  
Universitatea Tehnică Gh. Asachi – Iași

**JOVAN STEPANOVIĆ, DRAGAN RADIVOJEVIĆ, VASILJE PETROVIĆ,  
CARISA BESIC**  
Proiectarea caracteristicilor de deformare a firelor de lână unice  
și răsucite 99–105

**CAI GUANG MING, YU WEIDONG**  
Studierea proprietăților și a procesului de realizare a materialelor  
aramidice de înaltă performanță 106–111

**AURELIA GRIGORIU, CRISTINA RACU,  
RODICA MARIANA DIACONESCU, ANA-MARIA GRIGORIU**  
Modelarea procesului simultan de filare umedă-grefare a fibrelor  
de cânepă destinate textilelor medicale 112–116

**DENIZ DURAN, SEHER PERINCEK**  
Efectul diferiților parametri de producție asupra proprietăților fizice  
ale neșesutelor polipropilenice, filate din topitură 117–123

**SABINA OLARU, ADRIAN SĂLIȘTEAN, CLAUDIA NICULESCU,  
CONSTANTIN-CRISTIAN MATEŢCIUC, MIRELA TEODORESCU**  
Modele de optimizare a procesului de fabricație a parașutelor 124–128

**LUMINIȚA CIOBANU, CĂTĂLIN DUMITRAȘ, FLORIN FILIPESCU**  
Abordarea sistemică a proiectării tricotelurilor cu arhitectură  
tridimensională. Partea I 129–133

**ALEXANDRA ENE, CARMEN MIHAI, EMILIA VISILEANU,  
ALEXANDRU NICODIN, MIHAI CIOCOIU**  
Analiza curgerii sângelui prin implanturi cardiovasculare,  
în mișcarea laminară 134–139

**DOCUMENTARE** 140

**CRONICĂ** 111, 144

Recunoscută în România, în domeniul științelor ingineresti, de către  
Consiliul Național al Cercetării Științifice din Învățământul Superior  
(C.N.C.S.I.S.), în grupa A /

Acknowledged in Romania, in the engineering sciences domain,  
by the National Council of the Scientific Research from the Higher Education  
(CNCSIS), in group A

JOVAN STEPANOVIĆ,  
DRAGAN RADIVOJEVIĆ,  
VASILJE PETROVIĆ,  
CARISA BEŠIĆ

**Projecting of deformation characteristics of single and twisted wool yarns**

**Die Projektierung der Verformungseigenschaften von Einzel- und Twisted Wollgarne**

99

CAI GUANG MING,  
YU WEIDONG

**Investigation on the fabrication and properties of high performance aramid fabrics**

**Die Untersuchung der Eigenschaften und des Fertigungsprozesses der Aramid-Materialien hoher Leistung**

106

AURELIA GRIGORIU,  
CRISTINA RAČU,  
RODICA MARIANA DIACONESCU,  
ANA-MARIA GRIGORIU

**Modelling of the simultaneous wet spinning-grafting process of hemp fibres meant for medical textiles**

**Die Modellierung des simultanen Nassspinn-Pfropfprozesses der Hanffaser bestimmt für medizinische Textilien**

112

DENIZ DURAN,  
SEHER PERİNCEK

**The effect of various production parameters on the physical properties of polypropylene meltblow nonwovens**

**Effekt der verschiedenen Produktionsparameter auf die physische Eigenschaften der polypropylenischen Spinnvliesstoffe**

117

SABINA OLARU,  
ADRIAN SĂLIȘTEAN,  
CLAUDIA NICULESCU,  
CONSTANTIN-CRISTIAN MATENCIUC,  
MIRELA TEODORESCU,

**Optimization models of parachute manufacture process**

**Optimierungsmodelle für den Fertigungsprozess der Fallschirme**

124

LUMINIȚA CIOBANU,  
CĂTĂLIN DUMITRAȘ,  
FLORIN FILIPESCU

**Systemic approach to the design of knitted fabric with a three dimensional architecture. Part I**

**Der systematische Ansatz des Entwurfs der Gewirke mit 3D-Architektur. I. Teil**

129

ALEXANDRA ENE,  
CARMEN MIHAI,  
EMILIA VISILEANU,  
ALEXANDRU NICODIN,  
MIHAI CIOCOIU

**Analysis on the blood flow through the cardiovascular implants in the laminar motion**

**Die Analyse des Blutflusses durch Herz-Kreislaufimplante, in laminarer Bewegung**

134

DOCUMENTARE

**Documentation**

**Dokumentation**

140

CRONICĂ

**Chronicles**

**Chronik**

111, 144

Referenții articolelor publicate în acest număr al revistei INDUSTRIA TEXTILĂ/  
*Scientific reviewers for the papers published in this number:*

Cerc. șt. gr. II dr. ing./Senior researcher dr. eng. CARMEN MIHAI

Cerc. șt. gr. II ing./Senior researcher eng. MARIA DAN

Cerc. șt. gr. III drd. ing./Senior researcher eng. DOINA TOMA

Cerc. șt. gr. III/Senior researcher eng. GHEORGHE NICULA

Cerc. șt. drd. ing./Senior researcher eng. ADRIAN SĂLIȘTEAN

Cerc. șt. drd. mat./Senior researcher mat. MIHAI STAN

# Projecting of deformation characteristics of single and twisted wool yarns

JOVAN STEPANOVIĆ  
DRAGAN RADIVOJEVIĆ

VASILJE PETROVIĆ  
CARISA BEŠIĆ

## REZUMAT – ABSTRACT – INHALTSANGABE

### Proiectarea caracteristicilor de deformare a firelor de lână unice și răsucite

Determinarea valorilor limită ale sarcinii la care este supus firul pe parcursul prelucrării acestuia este o condiție preliminară pentru o reglare corectă a procesului, dar și pentru menținerea calității firului. Utilizând datele experimentale, modelul Berejev a fost modificat, astfel încât să poată fi proiectate forțele la rupere ale firelor de lână pieptănată de 18 tex și 32 tex. S-a obținut o ecuație prin derivare pentru proiectarea forțelor la rupere a firelor răsucite de 18 x 2 tex și 32 x 2 tex. S-au analizat elasticitatea, punctele de elasticitate maximă și punctele la rupere ale firelor unice de 21, 23 și, respectiv, 25 tex, și ale celor răsucite. Pe baza rezultatelor experimentale și a ecuațiilor teoretice, s-au stabilit relațiile matematice de proiectare a forțelor, alungirilor, limitelor de elasticitate, punctelor de elasticitate maximă și a celor de rupere ale firelor de lână unice și răsucite, oferind posibilitatea predicției comportamentului acestora pe parcursul prelucrării ulterioare.

Cuvinte-cheie: fir, lână, deformare, forță, alungire, elasticitate

### Projecting of deformation characteristics of single and twisted wool yarns

Determination of yarn load limit values during its processing is a precondition for correct process adjustment and also for maintaining yarn quality. Using experimental data, Berejev's model was modified in such way as to enable the projecting of the breaking forces of worsted wool yarns with linear densities of 18 tex to 32 tex. An equation for projecting breaking forces of twisted yarns with 18 x 2 tex and 32 x 2 tex was derived. The elasticity, elasticity limits and yield point limits of single yarns with 21 tex, 23 tex and 25 tex, as well as their more complex twisted structures were analyzed. Based on experimental results and theoretical equations, real mathematical relationships were established, enabling projecting of forces, elongations, elasticity limits, yield and breaking points of single and twisted wool yarns, which offers a possibility to predict yarn behavior during subsequent processing.

Key-words: yarn, wool, deformation, force, elongation, elasticity

### Der Entwurf der Verformungseigenschaften der Einzel- und Zwirnwollgarne

Die Bestimmung der Fadenbelastungsgrenzwerte während der Bearbeitung ist eine Vorbedingung für eine korrekte Prozessregelung, als auch für die Einhaltung der Garnqualität. Durch Anwendung der experimentellen Daten wurde das Berejev-Modell modifiziert, so dass die Bruchkräfte der gekämmten Wollgarne von 18 tex und 32 tex entworfen werden könnten. Es wurde durch Ableitung eine Gleichung erhalten für den Entwurf der Zwirngarn-Bruchkräfte von 18 x 2 tex und 32 x 2 tex. Es wurde die Elastizität, die Elastizitätshochpunkte sowie die Bruchpunkte der Einzelgarne für 21, 23, und entsprechend 25 tex, sowie der Zwirngarne, analysiert. Aufgrund der experimentellen Ergebnisse und der theoretischen Gleichungen, wurden mathematische Beziehungen für den Entwurf der Kräfte, der Dehnungen, der Elastizitätsgrenzen, der Elastizitätshochpunkte und der Bruchelastizitätspunkte der Einzel- und Zwirnwollgarne ermittelt, indem die Vorhersage deren Verhaltens während der nachträglichen Bearbeitung ermöglicht wurde.

Schlusswörter: Garn, Wolle, Verformung, Kraft, Dehnung, Elastizität

Staple yarns are complex textile materials, mainly consisting of fibers that are inhomogeneous regarding geometrical and mechanical characteristics, therefore, to define them a great number of parameters should be included.

Thus far, attempts to find formulas for projecting deformation characteristics of single and twisted yarns didn't give the best results. In the attempts two methods were applied: theoretical, resulting in more complex formulas, that again could not include all factors affecting yarn quality and calculation, and empirical, where the formula structure had a theoretical basis which included coefficients based on appropriate experimental data. Theoretical equations were developed on the basis of ideal mechanical models [1] and than coefficients [2] valid for the tested sample were introduced. The developed models analyzed the basic relationship force-strain, not taking into account characteristics of component fibers and, thereby, had only a limited application. Thus, an attempt was made, based on theoretical equations and real results, to define models for projecting the breaking characteristics of twisted yarns. Also, the relationships between breaking characteristics and parameters at elasticity limit and yield point were analyzed and equations for projecting forces and elongations at given limits were proposed, providing a possibility for prediction of yarn behavior

during subsequent manufacturing processes. Berejev's equation was used as a base model, (modified equation of A. N. Soloviev) [3]:

$$F_{rs} = F_{rf} \cdot K_v \cdot \left( 0,018 - 0,062 \cdot \sqrt{\frac{T_{ff}}{T_{ts}}} \right) \cdot K_a \cdot \eta \quad [\text{cN} / \text{tex}] \quad (1)$$

where:

$F_{rs}$  – is the relative breaking force of the single yarns, cN/tex;

$F_{rf}$  – the mean value of the fiber relative breaking force, cN/tex;

$K_v$  – the wool quality according to Bradford classification;

$T_{ff}$  – the fiber linear density, tex;

$T_{ts}$  – the single yarn linear density, tex;

$K_a$  – the twisting correction factor;

$\eta$  – the coefficient dependent on the state of equipment,  $\eta = 1$ .

During the processing of single phase twisted yarn with twisting direction opposite to the twists of the component yarns (twisted yarn ZS), these components experience an unwinding, and the cross section of the twisted yarn becomes a circular form. The properties of

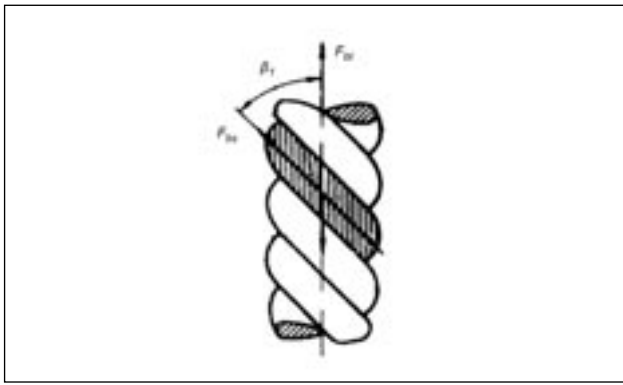


Fig. 1. Model of the twisted yarn

such twisted yarn depend on the properties of its component fibers and also on the intensity of twisting during spinning and subsequent twisting [4]. By straining of single phase twisted yarn ZS, made of  $n$  component yarns positioned at an  $\beta_1$  angle against the axis of the twisted yarn (fig. 1), its breaking force,  $F_{bt}$  can be defined with the following expression 4:

$$F_{bt} = F_{bs} \cdot n \cdot \cos \beta_1 \quad [\text{cN / tex}] \quad (2)$$

where:

- $F_{bt}$  is the breaking force of twisted yarn ZS, cN;
- $F_{bs}$  – the breaking force of single yarns within the twisted yarn, cN;
- $n$  – the number of single yarns in the twisted yarn;
- $\beta_1$  – the angle of single yarns to the axis of the twisted yarn.

The angle of the single yarns against the axis of the twisted yarn can be calculated from the following equation 4:

$$\beta_1 = \arctg \left( \pi \cdot d_s \cdot T_t \cdot 10^{-3} \right) \quad [^\circ] \quad (3)$$

where:

- $d$  is the diameter of single yarn in the twisted yarn, mm;
- $T_t$  – the number of twists of the twisted yarn,  $\text{m}^{-1}$ .

With the aim to develop an equation for projecting the breaking forces depending on fiber characteristics, Berejev's model (1) was included in the equation (2). Thus, equation (2) becomes:

$$F_{bt} = F_{rf} \cdot K_v \cdot \left( 0,018 - 0,062 \cdot \sqrt{\frac{T_{tf}}{T_{ts}}} \right) \cdot K_a \cdot \eta \cdot T_{ts} \cdot n \cdot \cos \beta_1 \quad [\text{cN}] \quad (4)$$

The value of the twisting correction factor,  $K_a$ , is defined depending on the single yarn twisting factors,  $a_m$  [3]. However, the value of parameter  $K_a$  is changed in the structure of the twisted yarn. Moreover, the equation for projecting the breaking force does not take into account friction forces between single yarns nor the friction forces between the fibers of component yarns. It should not be neglected that at twisted yarn breaking, the angle that single yarns have against the axis of the twisted yarn is at the minimum value. All this shows that the above equation could not be applied for a precise projecting of the twisted yarns breaking forces. There-

fore, the correction coefficient  $k_1$ , formed on the bases of real and calculated values of twisted yarns breaking forces, is included in equation 4, in order to obtain an equation applicable in real conditions.

Projecting of breaking elongation of twisted yarn represents a specific problem. There are a number of papers dealing with breaking elongations of twisted and single yarns. Mostly they propose empirical formulas. For this work the following formula is chosen [3]:

$$\varepsilon_{bt} = 0.9 \sqrt{T_{ts}} + 0.75 \cdot 10^{-3} \cdot \sqrt[3]{n \cdot T_{ts}} \cdot \alpha_t^2 \quad [\%] \quad (5)$$

where:

$\alpha_t$  is the twisting coefficient of the twisted yarns on the length of 1 cm.

In addition to breaking characteristics, the elasticity limits and yield points are essential characteristics of textile materials. Knowing the mentioned values, yarn behavior during processing into its more complex structures could be simulated. Moreover, these parameters define the forces which yarns could be subjected to during processing without affecting their quality significantly.

R. Meredith and M. J. Copland [5] suggested graphic methods for determination of yield points. However, modern software provides means of converting the  $F$ - $\varepsilon$  plot to an adequate function and to define the elasticity limits and yield points by analyzing this function [6, 7, 8].

## MATERIALS AND METHODS

Materials for experiments consisted of wool yarns spun by worsted method. One hundred and fourteen lots of twisted yarns with linear densities ranging from 18 x 2 tex to 32 x 2 tex ( $350 \text{ m}^{-1}$  to  $650 \text{ m}^{-1}$ ) were prepared. Parameters of all single yarn lots were used to modify Berejev' equation and to develop a model for projecting breaking forces of twisted yarns. In order to analyze elasticity and yield point limits, seventeen lots of various single yarns (Z) with linear densities of 21 tex ( $594.5 \text{ m}^{-1}$  –  $631.0 \text{ m}^{-1}$ ), 23 tex-a ( $556.0 \text{ m}^{-1}$  –  $626.0 \text{ m}^{-1}$ ) and 25 tex-a ( $554.0 \text{ m}^{-1}$  –  $600.0 \text{ m}^{-1}$ ) were selected. Twisted yarns were formed by two-for-one twisting method. In rewinding and twisting processes the forces inducing yarn tension were measured using electronic tensiometer type DTFX 200. For producing twisted yarns, lots of rewound yarns that had tension forces lower than forces at elasticity limit were selected. Moreover, tension forces in the twisting process were measured and it was found that they were largely lower than the forces at elasticity limits for twisted yarns analyzed, i.e. they were in the range of 24.3 cN to 64.5 cN. Herewith, the effect of tension force on possible plastic deformations of yarn was reduced to a minimum, whereby one of significant factors, that could affect results, was eliminated.

The breaking characteristics of experimental material (fig. 2) were measured on "USTER TENSORAPID 4" dynamometer (DIN 53384). Each of the  $F$ - $\varepsilon$  curves was formed on the basis of 20 single measurements (fig. 2). By using the software "REPAPP-UST 4", the typical curve for each yarn batch was derived and then converted to suitable function,  $F(\varepsilon)$ .

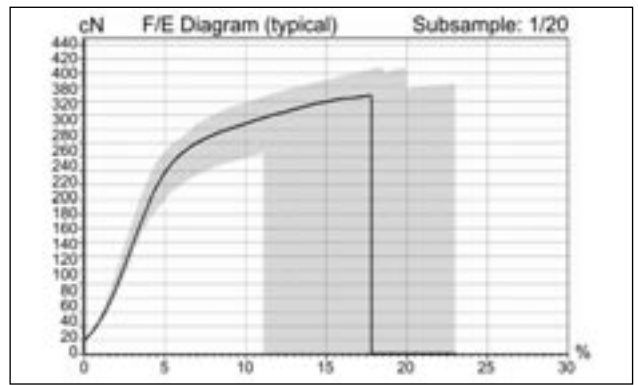
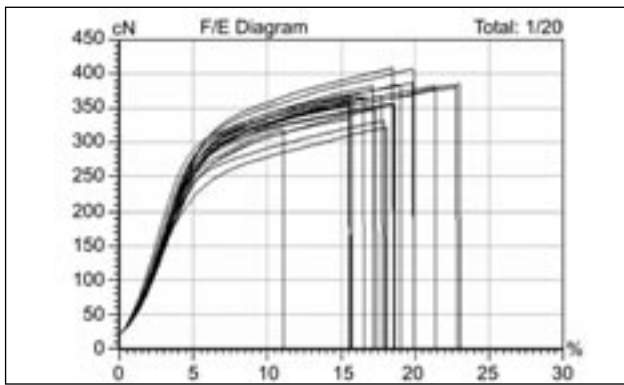


Fig. 2. Curves  $F$ - $\varepsilon$  recorded on "Uster Tensorapid 4" dynamometer

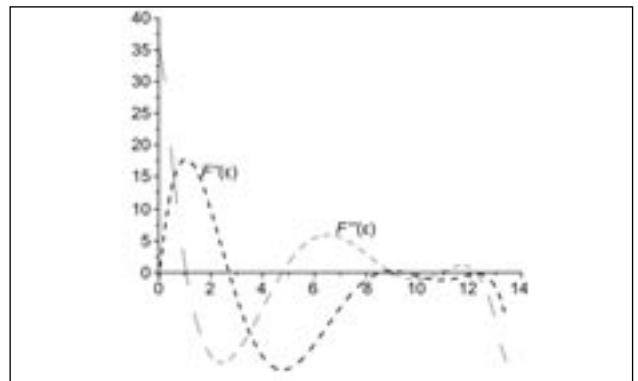
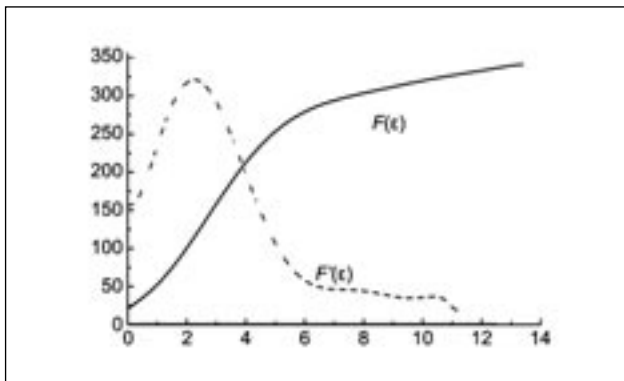


Fig. 3. First, second and third derivative of the  $F(\varepsilon)$  function, for the yarn with linear density of 21 x 2 tex

Analyzing the  $F(\varepsilon)$  functions, by using appropriate software, values were evaluated for the forces and relative elongations at elasticity limits,  $F_e$  and  $\varepsilon_e$ , of the wool twisted yarns, maximum of  $F'(\varepsilon)$  curve, i.e.  $F''(\varepsilon) = 0$  (fig. 3) [6, 7, 8]. Also, evaluated were the values of forces and relative elongations at yield points,  $F_y$ , where the first permanent deformation appears after the elasticity limit and they are numerically determined at the minimum point of the second derivative of  $F$ - $\varepsilon$  curve where  $F''(\varepsilon) = 0$  (fig. 3) [6–13].

The behavior of textile materials under low loads is mainly elastic. The ultimate load under which the material shows elastic properties of solids is called elasticity limit – the first derivative maximum of the  $F(\varepsilon)$  function. The further increasing of tension brings about certain fiber migrations in the yarn, resulting in a permanent deformation defined by the yield point – the second derivative minimum of the  $F(\varepsilon)$  function (fig. 3). Increasing the load over yield point causes significant deformations of yarn structure so the yield point represents a limit of permitted load the yarn may be subjected to in subsequent processing. Therefore, the aim of this work is to set up equations for predicting the permitted loads of single and twisted wool yarns, depending on their structural and constructive solutions.

## RESULTS AND DISCUSSIONS

Comparing breaking forces of the single yarns analyzed with their projected values according to equation (1), it was concluded that actual results deviate from theoretical values. Thus, equation (1) was corrected using actual values of parameters for the analyzed yarns, an equation form being obtained, which could be applied in real conditions:

$$F_{bs} = k_1 \cdot F_{rf} \cdot K_v \cdot \left( 0.018 - 0.062 \cdot \sqrt{\frac{T_{rf}}{T_{ts}}} \right) \cdot K_\alpha \cdot \eta \cdot T_{ts} \quad [\text{cN}] \quad (6)$$

To project the breaking elongation of single yarns, an empirical formula (7) was created, which relates the breaking elongation of single wool yarns with the fiber number over the cross section and the coefficient of the yarn twist number.

$$\varepsilon_{bs} = k_2 \cdot (0.004\alpha_{\text{tex},s} + 0.138N_{fs} - 3.695) \quad [\%] \quad (7)$$

where:

$\varepsilon_{bs}$  – is the breaking elongation of yarns, %;

$k_2$  – the correction coefficient of the breaking elongation;

$\alpha_{\text{tex},s}$  – the coefficient of the yarn twist number;

$N_{fs}$  – the number of fibers over the yarn cross section.

In figure 4 histograms for participation of elasticity limit and yield point forces to the yarn breaking forces are shown.

Figure 5 shows participations of elasticity limit and yield point elongations to breaking elongations.

The results obtained show that the elasticity limit force of single wool yarn participates to the breaking force with 16.856% to 29.929%, while the yield point force participation to the breaking force is 49.505% to 76.137%. Furthermore, the elasticity limit elongation of the single yarn participates with 6.389% to 9.307% and yield point elongation participates with 21.272% to 30.214% to the breaking elongation. Figure 6 shows the relationship between the elasticity limit, yield point and breaking forces of the wool yarns.

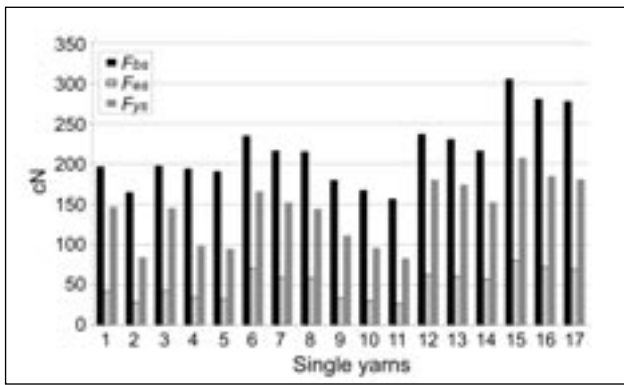


Fig. 4. The participation of elasticity limit and yield point forces to the yarn breaking forces:  $F_{bs}$  – breaking force;  $F_{es}$  – force at elasticity limit;  $F_{ys}$  – force at yield point

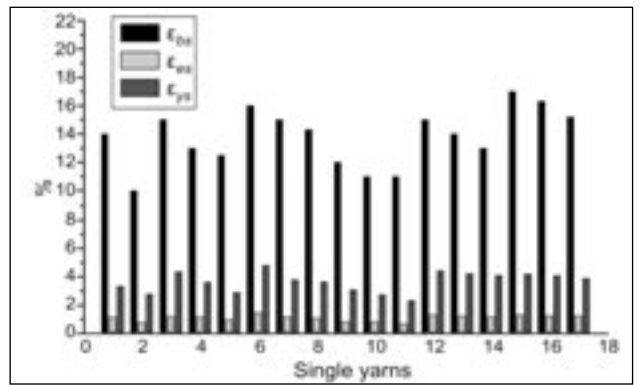


Fig. 5. Participation of elasticity limit and yield point elongation to the breaking elongations:  $\epsilon_{bs}$  – breaking elongation;  $\epsilon_{es}$  – elongation at elasticity limit;  $\epsilon_{ys}$  – elongation at yield point

The relationship between the breaking elongations and elongations at elasticity limits and yield points is shown in figure 7.

Based on the results obtained, equations for projecting forces at elasticity limits and yield points of analyzed yarns were derived:

$$F_{es} = k_1 \cdot k_3 \cdot F_{ff} \cdot K_v \left( 0.018 - 0.062 \cdot \sqrt{\frac{T_{ff}}{T_{ts}}} \right) \cdot K_\alpha \cdot \eta \cdot T_{ts} \quad [\text{cN}] \quad (8)$$

$$F_{ys} = k_1 \cdot k_4 \cdot F_{ff} \cdot K_v \left( 0.018 - 0.062 \cdot \sqrt{\frac{T_{ff}}{T_{ts}}} \right) \cdot K_\alpha \cdot \eta \cdot T_{ts} \quad [\text{cN}] \quad (9)$$

where:

$k_3$  is the correction coefficient of the elasticity limit force for the single yarns;

$k_4$  – the correction coefficient of the yield point force for the single yarns.

Based on the results obtained, equations for projecting elongations at elasticity limits and yield points of wool yarns were derived:

$$\epsilon_{es} = k_2 \cdot k_5 \cdot (0.004\alpha_s + 0.138 \cdot N_{fs} - 3.695) \quad [\%] \quad (10)$$

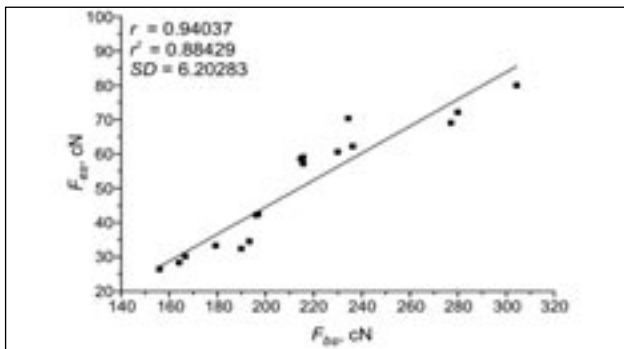
$$\epsilon_{ys} = k_2 \cdot k_6 \cdot (0.004\alpha_s + 0.138 \cdot N_{fs} - 3.695) \quad [\%] \quad (11)$$

where:

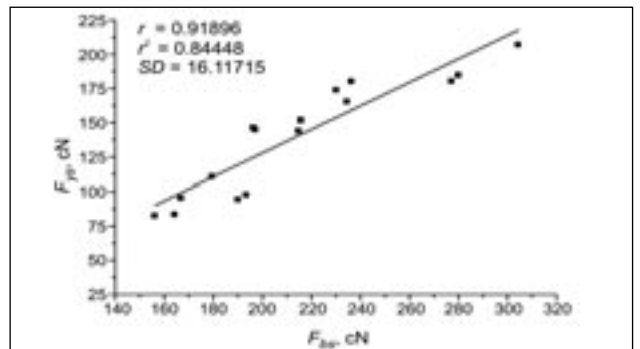
$k_5$  is the correction coefficient of the elasticity limit elongation for the single yarns;

$k_6$  – the correction coefficient of the yield point elongation for the single yarns.

Coefficients  $k_1$ ,  $k_2$ ,  $k_3$ ,  $k_4$ ,  $k_5$  and  $k_6$ , defined for all types of single yarns, are statistically processed and shown in table 1.

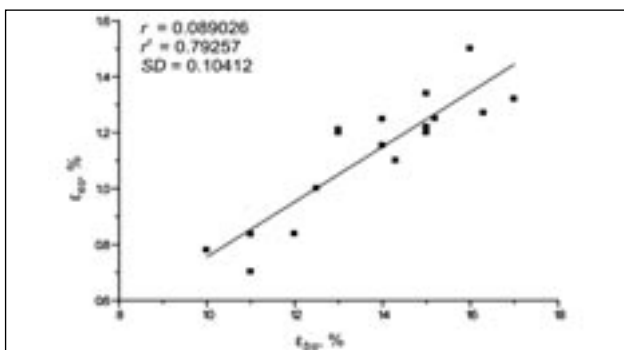


a

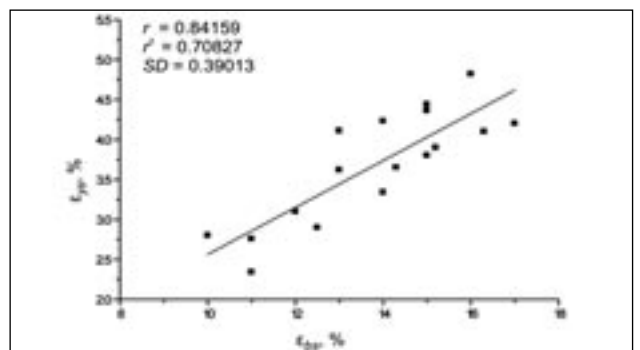


b

Fig. 6. Relationship between the breaking forces and forces at elasticity limits (a) and yield points (b) of the single yarns



a



b

Fig. 7. Relationship between the breaking elongations and elongations at elasticity limits (a) and yield points (b) of the yarns

VALUES OF COEFFICIENTS $k_1, k_2, k_3, k_4, k_5$ and $k_6$						
Parameter	$k_1$	$k_2$	$k_3$	$k_4$	$k_5$	$k_6$
$\bar{k}$	0.93459	0.93135	0.22842	0.64574	0.0814	0.26592
$\sigma$	0.05979	0.06212	0.045	0.09229	0.00815	0.0284
$CV$	6.39745	9.89101	19.700	14.29212	10.01228	10.6799
$P_{gg}$ (reliable 95%)	0.01097	0.00717	0.02139	0.04387	0.00387	0.0135
$\bar{k} + P_{gg}$	0.94556	0.93852	0.24981	0.68961	0.08527	0.27942
$\bar{k} - P_{gg}$	0.92362	0.92418	0.20703	0.60187	0.07753	0.25242

Table 2

VALUES OF COEFFICIENTS $k_7, k_8, k_9, k_{10}, k_{11}$ and $k_{12}$						
Parameter	$k_7$	$k_8$	$k_9$	$k_{10}$	$k_{11}$	$k_{12}$
$\bar{k}$	0.87295	2.61477	0.40296	0.69187	0.14299	0.26824
$\sigma$	0.08235	0.21889	0.09038	0.06437	0.01825	0.02208
$CV$	9.43352	8.37129	22.4290	9.30377	12.7631	8.23143
$P_{gg}$ (reliable 95%)	0.01511	0.04018	0.01659	0.01181	0.00335	0.00405
$\bar{k} + P_{gg}$	0.8806	2.6549	0.41955	0.70368	0.14634	0.27229
$\bar{k} - P_{gg}$	0.85784	2.57459	0.38637	0.68006	0.13964	0.26419

Analyzing the real results for the breaking forces of wool twisted yarns and their projected values, according to equation (4), it was found that real results differ from theoretical ones. Thus, equation (4) was corrected using real parameter values to obtain a form that could be employed under real conditions:

$$F_{bt} = k_1 \cdot k_7 \cdot F_{rf} \cdot K_v \cdot \left( 0.018 - 0.062 \cdot \sqrt{\frac{T_{ff}}{T_{ts}}} \right) \cdot K_\alpha \cdot \eta \cdot T_{ts} \cdot n \cdot \cos \beta_1 \quad [\text{cN}] \quad (12)$$

where:

$k_7$  is the correction coefficient of the twisted-yarn breaking force.

By introducing real data to equation (5) it was also found that the results obtained differ from real breaking elongations values. Therefore, using real results, a correction factor is included in equation (5) to obtain the following:

$$\varepsilon_{bt} = k_8 \cdot \left( 0.9 \sqrt{T_{ts}} + 0.75 \cdot 10^{-3} \cdot \sqrt[3]{n \cdot 12 \sqrt{T_{ts}}} \cdot \alpha_t^2 \right) [\%] \quad (13)$$

where:

$k_8$  is the correction coefficient of the twisted-yarn breaking elongation.

Coefficients  $k_7$  and  $k_8$  were statistically processed, as shown in table 2. Figure 8 shows the histograms for the participation of elasticity limit and yield point forces to the breaking forces of the twisted yarns.

The results (fig. 8) show that elasticity limit force of wool twisted yarn participates to the breaking force with 21.1124% to 54.664%, and yield point force participation to breaking force is 54.378% to 82.569%. Furthermore, elasticity limit elongation of single yarn participates with 10% to 17.3469% and yield point elongation participates with 22.450% to 31.724% to the breaking elongation. The parameters shown are changed with twist number, where the participation of analyzed parameters increases with twist number of twisted yarn. Based on the results obtained, the rela-

tionships between real breaking forces, elasticity limit and yield point forces are shown in figure 9.

Using the relationships obtained the equations for projecting forces at elasticity limit and yield point for analyzed twisted wool yarns could be proposed:

$$F_{et} = k_1 \cdot k_7 \cdot k_9 \cdot F_{rf} \cdot K_v \cdot \left( 0.018 - 0.062 \cdot \sqrt{\frac{T_{ff}}{T_{ts}}} \right) \cdot K_\alpha \cdot \eta \cdot T_{ts} \cdot n \cdot \cos \beta_1 \quad [\text{cN}] \quad (14)$$

$$F_{yt} = k_1 \cdot k_7 \cdot k_{10} \cdot F_{rf} \cdot \left( 0.018 - 0.062 \cdot \sqrt{\frac{T_{ff}}{T_{ts}}} \right) \cdot K_\alpha \cdot T_{ts} \cdot \eta \cdot n \cdot \cos \beta_1 \quad [\text{cN}] \quad (15)$$

where:

$k_9$  is the correction coefficient of the elasticity limit force for the twisted yarns;

$k_{10}$  – the correction coefficient of the yield point force for the twisted yarns.

Elongations at elasticity limit and yield point could also be presented with the equations:

$$\varepsilon_{et} = k_8 \cdot k_{11} \cdot \left( 0.9 \sqrt{T_{ts}} + 0.75 \cdot 10^{-3} \cdot \sqrt[3]{n \cdot 12 \sqrt{T_{ts}}} \cdot \alpha_t^2 \right) [\%] \quad (16)$$

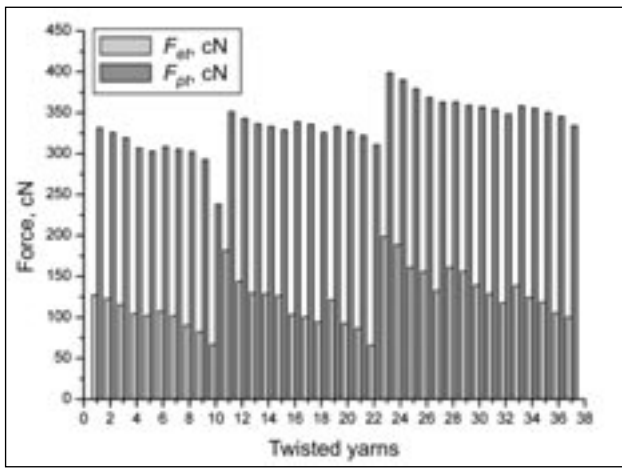
$$\varepsilon_{yt} = k_8 \cdot k_{11} \cdot \left( 0.9 \sqrt{T_{ts}} + 0.75 \cdot 10^{-3} \cdot \sqrt[3]{n \cdot 12 \sqrt{T_{ts}}} \cdot \alpha_t^2 \right) [\%] \quad (17)$$

where:

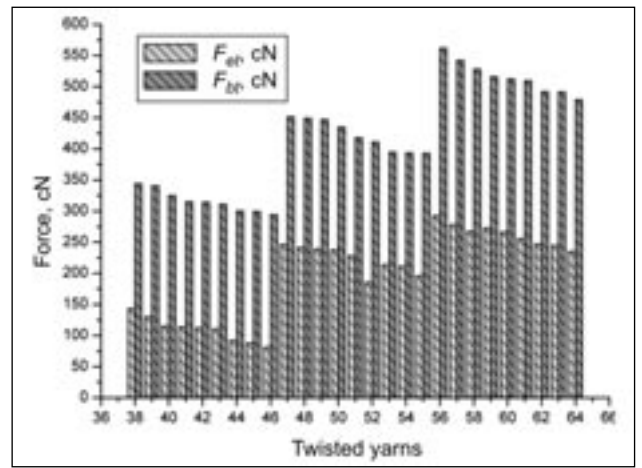
$k_{11}$  is the correction coefficient of the elasticity limit elongation for the twisted yarns;

$k_{12}$  – the correction coefficient of the yield point elongation for the twisted yarns.

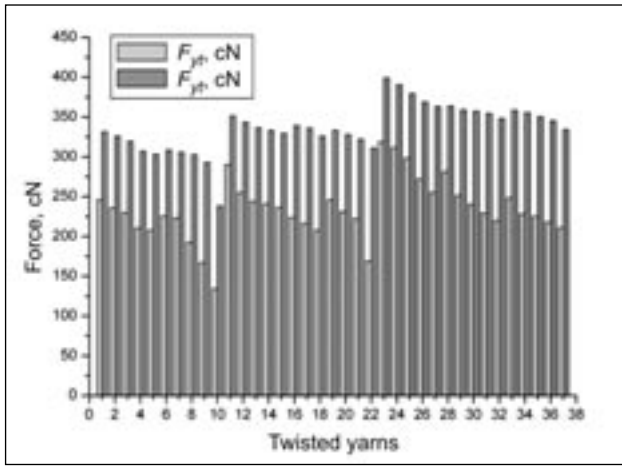
Coefficients  $k_7, k_8, k_9, k_{10}, k_{11}$  and  $k_{12}$  are defined for all types of analyzed twisted yarns, statistically processed and shown in table 2. Based on the obtained results, it can be concluded that there is a good cor-



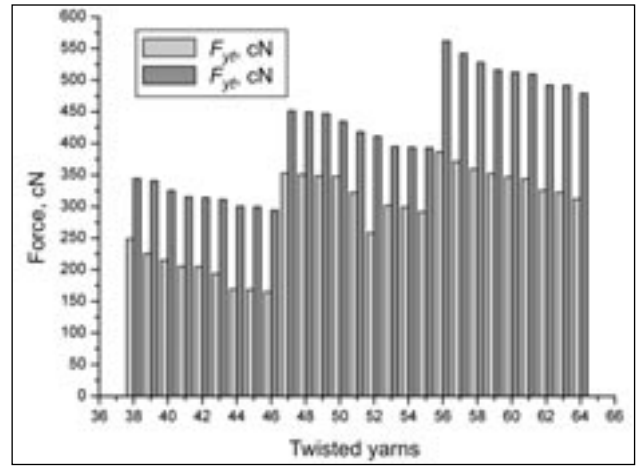
a



b



c



d

Fig. 8. Participation of elasticity limit (a, b) and yield point (c, d) to the breaking forces of the twisted yarns;  $F_{bt}$  – breaking force;  $F_{et}$  – force at elasticity limit;  $F_{yt}$  – force at yield point

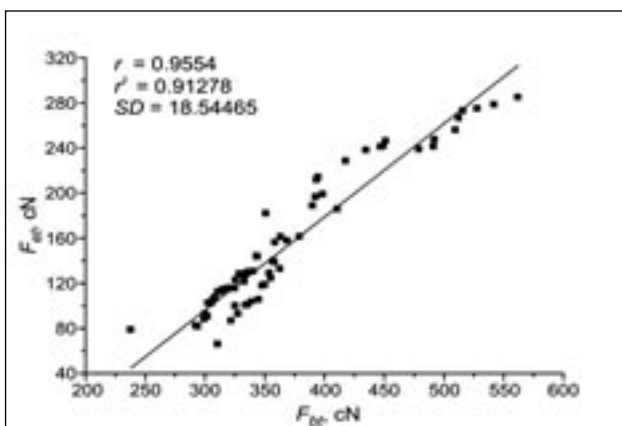
relation between the breaking forces, elasticity limit forces and yield point forces on one side, and the high values of the correlation coefficient, on the other side, for the single and the twisted wool yarns. Figure 10 shows the relationship between real breaking elongations and elongations at elasticity limit and yield point of twisted yarns.

The results also show a correct relationship between the breaking elongations, elongations at elasticity limits and yield points. The equations obtained in this way

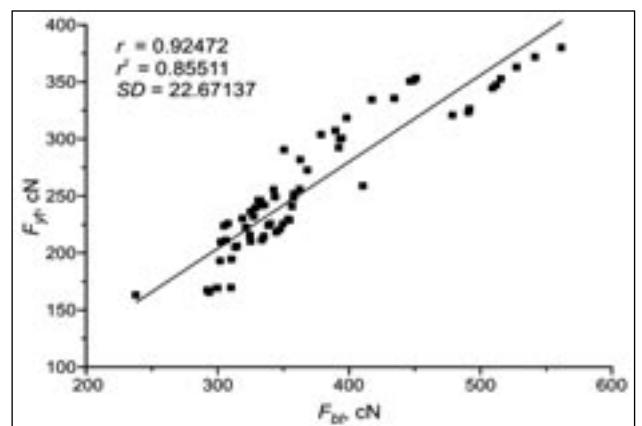
may be used with single and twisted yarns for projecting forces at elasticity limits, yield points and breaking. Therewith, loads permitted in subsequent processing can be projected without disturbing their quality performances.

## CONCLUSIONS

Deformation characteristics of twisted yarns depend on their structural and constructive solutions and on the

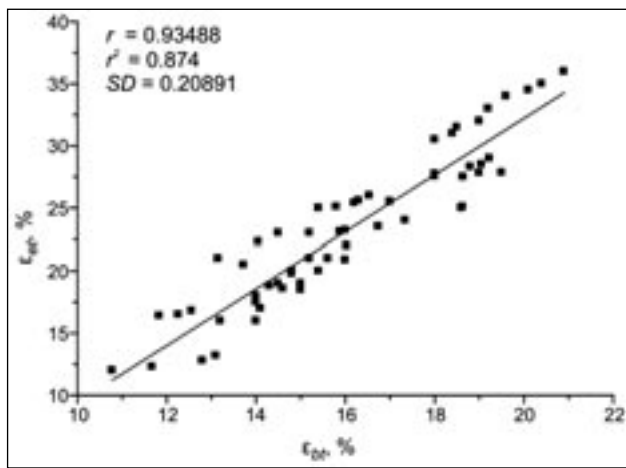


a

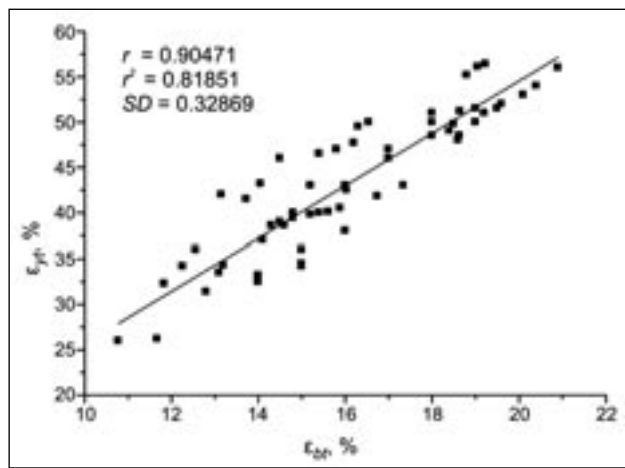


b

Fig. 9. Relationship between the breaking forces and elasticity limits forces (a) and yield points forces (b) of the twisted yarns



a



b

Fig. 10. Relationship between the breaking elongations and elongation at elasticity limit (a) and yield point (b) of the twisted yarns:  $\epsilon_{bt}$  – breaking elongation;  $\epsilon_{et}$  – elongation at elasticity limit;  $\epsilon_{yt}$  – elongation at yield point

technological parameters within the spinning, winding and twisting processes. Using geometrical model of twisted yarn, theoretical equations and experimental results, equations for projecting breaking forces and breaking elongations of single and twisted worsted wool yarns (18 tex to 32 tex, twist numbers  $430\text{ m}^{-1}$  to  $742.4\text{ m}^{-1}$ ) were derived. Moreover, results showed a high correlation between deformation characteristics that could link the parameters and suggest equations for projecting forces and elongations at elasticity limits and yield point of single yarns (21 tex, 23 tex and 25 tex, twist numbers  $554\text{ m}^{-1}$  to  $631\text{ m}^{-1}$ ) and twisted (21

$\times 2\text{ tex}$ ,  $23 \times 2\text{ tex}$  and  $25 \times 2\text{ tex}$ , twist numbers  $473\text{ m}^{-1}$  to  $592,2\text{ m}^{-1}$ ) wool yarns. The results also showed a high correlation of deformation characteristics providing the conditions to correlate parameters and propose equations for projecting forces and elongations at elasticity limits and yield points of wool yarns. The proposed equations can be applied for predicting loads permitted in processing of single and twisted wool yarns, without disturbing their quality parameters. This way, technical preparation of production can be simplified and improved, ensuring energy and raw material savings.

#### BIBLIOGRAPHY

- [1] Serwatka, A., Bruniaux, P., Frydrych, I. *New Approach to modeling the stress-strain curve of linear textile products. Part 1. Theoretical Considerations*. In: *Fibres & Textiles in Eastern Europe*, 2006, vol. 55, issue 1, p. 30
- [2] Serwatka, A., Bruniaux, P., Frydrych, I. *Modelling the stress-strain curve of textile products. Part 2. Simulation of Real Stress-strain Curves*. In: *Fibres & Textiles in Eastern Europe*, 2007, vol. 62, issue 3
- [3] Nikolić, M., Gregorič, A. *Teorija predelave vlakna, Fakulteta za naravoslovje in tehnologijo*. Univerza v Ljubljani, Ljubljana, 1987, p. 184
- [4] Koritzkii, K. I. *Inženernoe proektirovanje tekstilnih materialov*. Liogkaja Industrija, Moskva, 1971, p. 95
- [5] Gersak, J. *Study of the yield point of the thread*. In: *Clothing Sci. Technol.*, 1998, vol. 10, issue 3/4, p. 244
- [6] Bukošek, V. *Računalniško vrednotenje viskoelastičnih lasnosti vlakna*. In: *Tekstilec*, 1983, vol. 26, issue 12, p. 24
- [7] Geršak, J. *Rheological properties of threads. Rheological properties of threads*. In: *Clothing Sci. Technol.*, 1995, vol. 7, issue 2/3, p. 71
- [8] Stepanovic, J., Stamenkovic, M., Antic, B., Radivojevic, D. *Deformation characteristics of wool fabrics*. In: *Indian Text. Journal*, 1999, vol. 110, issue 11, p. 46
- [9] Radivojevic, D., Stamenkovic, M., Stepanovic, J., Trajkovic, D. *Yarn tension influence on deformation characteristics of wool type wound yarns*. In: *Materials Science*, 2002, vol. 8, issue 2, p. 196
- [10] Radivojevic, D., Stamenkovic, M., Stepanovic, J., Antic, B. *Influence of yarn tension in twisting on the yarn breaking characteristics*. In: *Fibres & Textiles in Eastern Europe*, 2001, vol. 32, issue 1, p. 20
- [11] Radivojevic, D., Stamenkovic, M., Stepanovic, J., Trajkovic, D. *Poly-cyclic mechanical deformations of unwound yarns*. In: *Fibres & Textiles in Eastern Europe*, 2002, vol. 37, issue 2, p. 18
- [12] Radivojevic, D., Stamenkovic, M., Stepanovic, J., Antic, B. *Poly-cyclic mechanical properties of twisted yarns*. In: *Vlakna à textil*, 2000, vol. 7, issue 1, p. 2
- [13] Stojiljkovic, T. D., Petrovic, V., Petrovic, D. M., Ujevic, D. *Defining the memory function for tension and deformation of linear textile products on the basis of their rheological models*. In: *Industria Textilă*, 2009, vol. 60, issue 6, p. 308

#### Authors:

JOVAN STEPANOVIĆ  
Faculty of Technology  
University of Niš  
Bulevar oslobođenja 124  
16000 Leskovac, Serbia  
e-mail: jovan64@yahoo.com  
DRAGAN RADIVOJEVIĆ  
High Technical School of Textile  
Leskovac, Serbia

VASILJE PETROVIĆ  
„Mihajlo Pupin“ Technical Faculty, Zrenjanin  
University of Novi Sad, Serbia  
CARISA BEŠIĆ  
Technical Faculty Čačak  
University of Kragujevac  
65 Svetog Save St., 32000, Serbia

# Investigation on the fabrication and properties of high performance aramid fabrics

CAI GUANG MING

YU WEIDONG

## REZUMAT – ABSTRACT – INHALTSANGABE

### Studierea proprietăților și a procesului de realizare a materialelor aramidice de înaltă performanță

În lucrare sunt prezentate două tipuri de materiale aramidice, realizate cu trei tipuri de legături. Datorită bunelor proprietăți mecanice, de rezistență la temperatură și stabilitate la radiații luminoase, aceste materiale sunt utilizate în industria aerospațială, militară și de îmbrăcăminte. În urma evaluării proprietăților de rezistență la abraziune și la tracțiune, s-a constatat că, în timpul procesului de țesere, fibra aramică prezintă un grad ridicat de degradare. De asemenea, au fost analizate caracteristicile de reflexie și transmisie, precum și efectul temperaturii asupra proprietăților la tracțiune. Studiul are ca scop optimizarea caracteristicilor de funcționalitate, securitate, rezistență și design ale materialelor destinate stratului exterior al echipamentelor de protecție.

Cuvinte-cheie: materiale aramidice, proprietăți, optimizare, utilizare

### Investigation on the fabrication and property of high performance aramid fabrics

The paper presents two types of aramid fibers achieved with three different weaves. Due to their good mechanical, light radiation stability and temperature-resistant properties, these materials are used in aerospace, military and clothing industries. The analysis of the tensile and abrasion resistance strength showed that, during the waving process, aramid fabrics have a high degree of degradation. The reflection and transmission features of the aramid fabrics, as well as the effect of temperature on the tensile properties of fabrics were also analyzed. The study aims to provide the optimization of functionality, security, stability, as well as the outer layer design characteristics of protective equipment.

Key-words: aramid fabrics, properties, optimization, utilization

### Die Untersuchung der Eigenschaften und des Fertigungsprozesses der Aramid-Materialien hoher Leistung

In der Arbeit werden zwei Typen von aramidischen Materialien vorgestellt, welche mit drei Bindungsarten fertiggestellt wurden. Dank der guten mechanischen Eigenschaften, des guten Temperaturwiderstandes und der Stabilität bei Lichtstrahlung, werden diese Materialien in der Luftfahrtindustrie, der Militärindustrie und der Bekleidungsindustrie angewendet. Als Folge der Bewertung der Eigenschaften betreff Abrieb- und Zugfestigkeit hat man festgestellt, dass im Laufe des Webprozesses, die aramidische Faser einen hohen Abnutzungsgrad aufweist. Es wurden gleichfalls die Eigenschaften betreff Reflexion und Transmission analysiert, sowie der Einfluss der Temperatur auf die Zugeigenschaften. Die Studie hat als Zweck die Optimisierung der Eigenschaften für Funktionalität, Sicherheit, Widerstand und Design der Materialien für die Aussenschicht der Protektionsausrüstungen.

Schlüsselwörter: Aramid-Materialien, Eigenschaften, Optimisierung, Anwendung

Aramid fabrics have good thermal and light stabilities, which are widely used in the aerospace, military and protective clothes, such as Kevlar and Nomex filaments made by DuPont. A basic requirement for the fabrics used in the military and aerospace fields is that the fabrics should have high mechanical properties. The fabrics are subjected to ageing and degradation when they are exposed to thermal and light radiation. Many studies have been conducted on the effects of sunlight and thermal exposure over polyamides. Singleton, Kunkel, and Sprague had indicated that the quantity of ultraviolet light, in the total light, and humidity are the key variables in the fiber photo-degradation [1]. M. Day had reported the effect of light on the flammability of Nomex fabric [2] and Genc studied the moisture sorption and thermal characteristics of aramid blend fabrics [3]. Under high temperature or exposure to UV radiations, degradation occurred on the aramid yarns and fabrics, which caused a decrease of the tensile properties. Previous studies on the influence of high temperature and ultraviolet radiation over the aramid durability and stability were focused on fibers and yarns, but less work was concerned with the fabric, or discussed about the fabrication of aramid fabrics and the damage of aramid fabrics in the weaving process. As the modulus is high and the elongation characteristics are low for the high performance products, it is easy to produce high tension in the yarn, leading to fiber

breaking in the waving process [4]. In this investigation, the fabrication of aramid yarns and fabrics was discussed, as well as the mechanical properties of the three fabric weaves and two types of fabric considered; it was also analyzed the damage properties these fabrics have in the weaving process. The two types of samples dealt with were subjected to high temperature, and the effects of temperature on the tensile properties were also discussed. In addition, the reflection and transmission properties were evaluated for three kinds of fabrics matching the interval between 250 and 2500 nm wavelength.

## FABRICATION OF THE ARAMID FABRIC

### Choice of fiber materials

A basic requirement for the fabric used in extreme conditions is that the materials have good flexibility and resistance to repeated fatigue. Only the high-performance fibers can satisfy those requirements. The glass fiber has high strength, heat resistance, but it is brittle [5]. The carbon fiber has high heat resistance, good resistance to chemical corrosion, small thermal shock, and low thermal expansion, but the fiber is easily brittle-damaged [6]. The high strength and high modulus density-polyethylene fiber has specific properties, as said, in terms of strength, modulus, softness and resistance to fatigue, but their heat resistance is poor [7]. In addition to aromatic polyamide fibers having the advantages

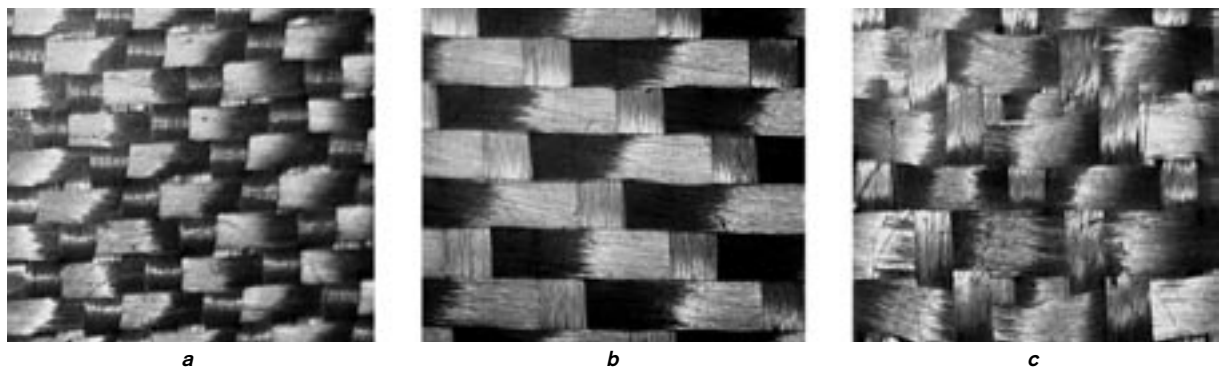


Fig. 1. Photos of the three types of fabric weave:  
a – broken twill; b – satin weave; c – fancy weave

Table 1

RAW MATERIALS			
Sample	Density, den	Breaking strength, cN	Breaking elongation, %
Kevlar 49 filament	200	3 925	3.65
Nomex filament	200	1 056.42	26.86

of a carbon fiber and the high strength and high modulus of a polyethylene one, these have stable thermal and mechanical properties, resistance to high temperature and resistance to flame [8]. Therefore, this paper chose as raw materials the Kevlar 49 and Nomex fiber of DuPont Company.

#### Fabrication of the yarn

Warp yarn and weft yarn suffer repeated bending, stretching and friction in the weaving process. Therefore, it requires the yarns to have good toughness, resistance to buckling and abrasion. The Kevlar fiber has a high strength and high modulus, and its tensile strength and strength uniformity can meet the requirements of weaving, but the buckling resistance and abrasion resistance are relatively weak, so the double-strand, low-twist yarn can be used. The Nomex fiber has great breaking elongation and flexibility, but the breaking strength is low. We made Nomex and the Kevlar filament compound by twisting and then formed the different raw-materials compound yarns. Table 1 shows the properties of these raw materials.

#### Fabrication of the fabric

Considering uniform and stable properties of the fabric weaves structure, three kinds of weave structures were designed in this paper. The first is a symmetry broken twill weave, which shows that the weave's point is symmetrical and uniform, figure 1a. The forces in all directions are steady, and the grip between yarns is better, but the weave structure is tight for this kind of weave, which is less favorable for the tear and stab purposes. The fabric tear strength depends primarily on the number of yarns in the stress area [9]. The interlacing frequency of yarns is relatively large, and the long-term floating relatively short. Therefore, the relative movement between the yarn and the yarn length of the force is quite small in this structural weave.

Secondly, in order to overcome the tight structure and improve the fabric flexibility, was considered the satin weave shown in figure 1b. The interweave points are

Table 2

GENERAL DETAILS OF THE SPECIMENS				
Item	Weave pattern	Fabric count, warp x weft ends.inch <sub>-1</sub>	Fabric thickness, mm	Fabric mass, g/m <sup>2</sup>
$B_1$	Pure broken twill	21 x 19	0.42	203.52
$S_1$	Pure satin weave	21 x 19	0.45	201.43
$F_1$	Pure fancy weave	21 x 19	0.44	201.53
$B_2$	Blended broken twill	21 x 19	0.42	205.42
$S_2$	Blended satin weave	21 x 19	0.47	202.43
$F_2$	Blended fancy weave	21 x 19	0.46	200.43
$B_3$	Blended broken twill	23 x 21	0.41	212.02

less and the flexibility of the weave structure is better, but the interweave points keep the direction, so the fabric symmetry is not obvious.

It was found that any one warp or weft yarn has only one interweave point in one weave circulation, figure 1a, b. Thereby, the distribution of long-term floating is uneven, as the interlacing point yarn fluctuated considerably, and the fiber damage is large in the weaving process. In order to achieve the softness and symmetry objective, it was then considered the fancy weave, as shown in figure 1c. The weave has a long float and a double-thick point, so the fabric will become softer, and the structure will finally get a good flexibility and stability.

In order to ensure a good abrasion resistance and softness, fabric should be as thin as possible, so these weaves are all in the zero-structure phase [10].

#### Experimental materials and instruments

The materials include the Kevlar 49 pure fabric and the Kevlar 49/Nomex blended fabric in three kinds of weaves, and all the fabrics were made of 200 denier filament yarns, Kevlar and Nomex. Material specifications are listed in table 2. The test instruments were WDW-20 tensile tester, Y522 disk surface grinding instrument, U-4100 spectrophotometer. The heat treatments were performed in a muffle furnace with a temperature treatment under 200°C.

## RESULTS AND DISCUSSIONS

#### Tensile properties and the damage analysis of the aramid fabric

The breaking strengths of the selected three kinds of fabric weaves are presented in tables 3 and 4. It is obvious that there is not much contrast between the

Table 3

TENSILE PROPERTIES OF THE PURE ARAMID FABRIC						
Weave pattern	Broken twill		Satin weave		Fancy weave	
	warp	weft	warp	weft	warp	weft
Breaking strength, $F/N$ , Average	2 538.36	3 248.32	2 542.33	3 236.58	2 567.43	3 252.79
CV	8.24	4.76	9.04	4.76	7.34	4.76
Breaking elongation, $\epsilon/\%$ , Average	5.22	4.98	5.23	5.03	5.4	5.35
CV	5.38	8.99	5.38	8.99	5.38	8.99

Table 4

TENSILE PROPERTIES OF THE PURE ARAMID FABRIC								
Weave pattern	Broken twill-1		Satin weave		Satin weave		Broken twill-2	
	warp	weft	warp	weft	warp	weft	warp	weft
Breaking strength, $F/N$ , Average	1 620.04	1 830.38	1 632.14	1 854.23	1 601.32	1 812.26	1 705.23	1 892.32
CV	4.17	2.5	3.87	3.88	2.45	6.44	8.24	4.76
Breaking elongation, $\epsilon/\%$ , Average	5.73	5.30	5.71	5.42	6.03	5.68	5.00	5.69
CV	6.37	1.79	2.55	3.48	2.79	2.43	5.38	8.99

different weave fabrics. Only the fancy weave has a larger breaking strength.

The strength in the warp direction is higher than that in the weft direction for the pure and the blended fabric. This is because the Kevlar fiber has high modulus and poor friction properties, and the warp yarns mechanical strength shows a greater loss in the process, which results in total fabric strength becoming lower.

As can be seen from tables 3 and 4, the breaking strength is stronger for the pure fabric than for the blended fabric. The reason is that the Nomex filament strength is lower than that of the Kevlar one. Yet, the breaking elongation of the blend fabric is higher than that of the pure fabric. This result can be explained by the properties of Nomex and Kevlar yarns, as the Nomex filament has a great breaking elongation. At the same time, it can be noted that the fabric breaking strength can be improved by increasing the fabric density.

For Kevlar, compared to the original filament and yarn, the strength loss rate was found to be 4.1%, and the elongation loss rate -4.7%, after the filament twisting to yarn, which indicates that the strength decreases and elongation increases when the original filament is

twisted, table 5. The Kevlar fiber strength loss may be due to the shear stress creating the Kevlar fiber axial slippage and due to the weakening occurring after twisting [11]. If the twist is small, the yarn damage can also be reduced. It was found that the strength loss rate of the Kevlar fabric reaches 35%, which is due to the Kevlar fiber elongation rate being low. When the yarns are subject to opening and severe beating, the yarns generate deformation during the weaving process. The loss rate in the warp direction is higher than in the weft direction. The main reason is that the buckling of the warp yarn is larger than for the weft yarn, and the warp yarns are subjected to a greater tension and repeated friction in the weaving process.

The strength loss rate of the blended fabrics is shown in table 6. The results reveal a 2.54% strength loss rate of the Kevlar/Nomex blend yarn, less than the strength loss rate of the original pure Kevlar filament twisted yarn. The loss rate for elongation is -31.23%, indicating that the exploitation of yarns mechanical properties can be increased by yarn blending and twisting.

The loss rate of the blend fabric is 28.37% in the warp direction, which is less than that of the pure fabric. This is mainly because the friction resistance of yarns im-

Table 5

DAMAGE ANALYSIS OF PURE KEVLAR FABRIC IN WEAVING PROCESS			
Materials	Index	Breaking strength, N	Breaking elongation rate, %
Filament	Average	78.5	3.65
Yarn	Average	75.55	3.82
	Loss rate, %	4.1	-4.7
Warp of fabric	Average	2 549.37	5.28
	Yarn relative loss rate, %	34.07	-38.22
	Total loss rate, %	35.01	-44.66
Utilization rate of the warp yarn, %		64.99	144.66
Weft of fabric	Average	3 245.9	5.12
	Yarn relative loss rate, %	9.6	-34.03
	Total loss rate, %	12.95	-40.27
Utilization rate of the weft yarn, %		87.05	140.27

Table 6

DAMAGE ANALYSIS OF KEVLAR/NOMEX BLENDING FABRIC IN WEAVING PROCESS			
Materials	Index	Breaking strength, N	Breaking elongation rate, %
Filament	Average	44.14	3.65
Yarn	Average	43.02	4.79
	Loss rate, %	2.54	-31.23
Warp of fabric	Average	1 617.18	5.28
	Yarn relative loss rate, %	28.37	-21.5
	Total loss rate, %	30.18	-59.45
Utilization rate of the warp yarn, %		69.82	159.45
Weft of fabric	Average	1 832.29	5.47
	Yarn relative loss rate, %	10.33	-14.2
	Total loss rate, %	12.6	-50
Utilization rate of the weft yarn, %		87.4	150

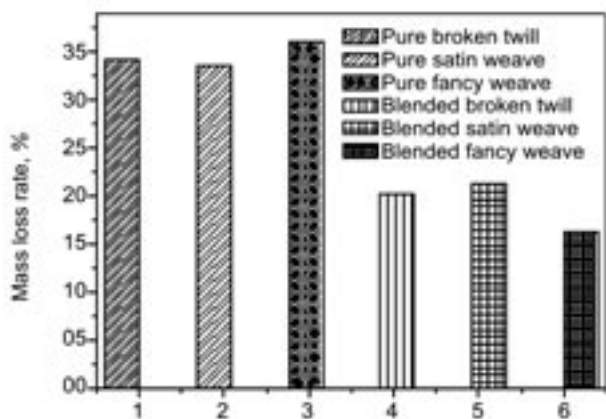


Fig. 2. Comparison of the abrasion resistance properties for the aramid fabrics

proves after blending. The warp direction subjected to repeated friction results into a high decrease of strength during the weaving process, strength that can be improved by increasing the friction performance of yarns.

From the analysis above, it can be found that there is still a large scope for fiber damage reduction in the weaving process and for such high-strength, low elongation fibers application rate improvement.

#### Wear resistance properties of the aramid fabric

In figure 2, we can find that the fabrics made of blended yarns have a better abrasion resistance than the pure fabrics, which have a great loss of mass. Because the Kevlar yarns have a great rigidity and brittleness, the Kevlar fiber is easy to rupture when the fabrics are worn. The Nomex yarn has great flexibility and wear resistance properties, the fabric wear resistance being improved by blending. The abrasion resistance difference is little between the different fabrics organizations.

#### Reflection and transmission properties of the aramid fabric

One of the requirements for a fabric with good protective features is that the absorption rate and transmission rate of the fabric should be as small as possible, while the reflectivity of light should be as large as possible. Spectral reflectance results of some different aramid fabrics are presented in figures 3 and 4;

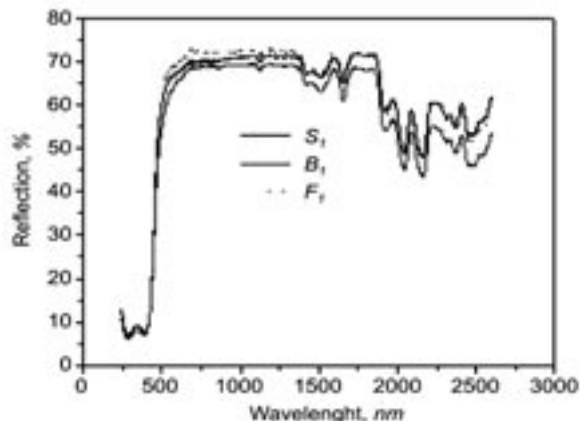


Fig. 3. The reflectance spectra between 250 to 2 500 nm

it is obvious that the reflectance curves of different fabrics have slightly changed throughout the full range of wavelengths, from 250 to 2 600 nm. All of the fabrics have a high reflectance, up to 70% between 800 nm and 1800 nm wavelength. The fancy weave and the satin weave are no different; the broken twill weave is at minimum. These happen because the reflection properties are affected by the surface roughness; the fancy and the satin weave fabrics have a long float, a small crossing point, great symmetry and plane, which lead to the higher reflectivity.

In figure 4, we can see that the Nomex/Kevlar blended fabric has a higher reflectivity than the Kevlar fabric in the entire wavelength spectrum. The result can be explained by the Nomex and Kevlar filament properties, as Nomex is white and Kevlar is yellow. Because white has a great reflectivity, the blended fabric has great reflection properties. Once the reflectance is increased, transmission and absorption rate will reduce. Therefore, we can improve the light resistance of the aramid fabric by a Kevlar/Nomex blending.

Figure 5 explains the transmission properties; we can find that the transmission is relatively low in ultraviolet spectra and that all of the three weaves are the same, but the transmission properties show a great difference between 800 nm and 1 800 nm wavelength. Figure 6 explains the transmission spectra between 250 to 2500 nm. The broken twill weave has the lowest transmission, while the fancy weave has the highest. Because the broken twill weave is rather compact and small

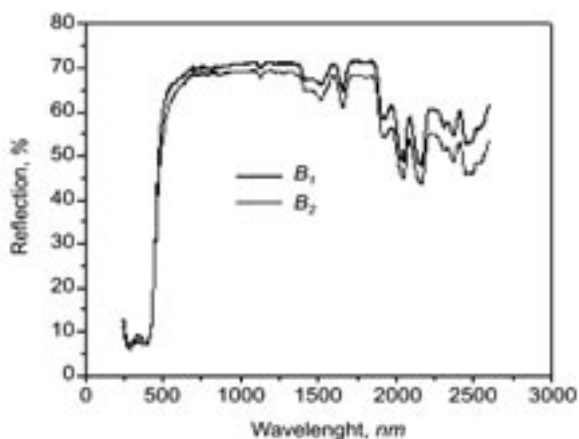


Fig. 4. The reflectance spectra between 250 to 2 500 nm

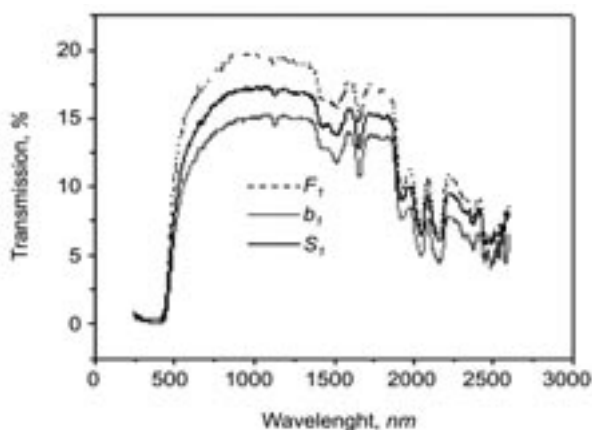


Fig. 5. The transmission spectra between 250 to 2 500 nm

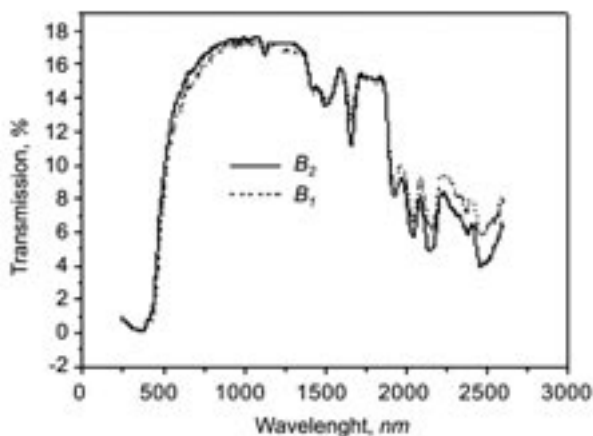


Fig. 6. The transmission spectra between 250 to 2500 nm

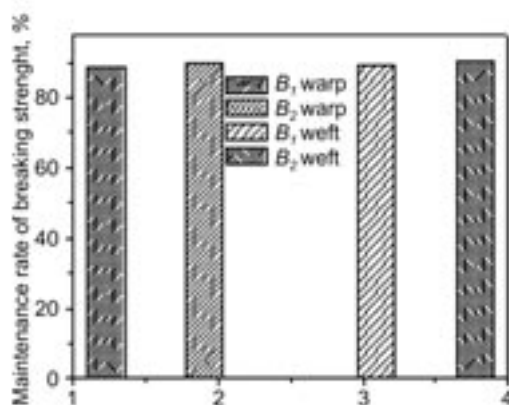


Fig. 7. The maintenance rate of the breaking strength under 200°C treatment

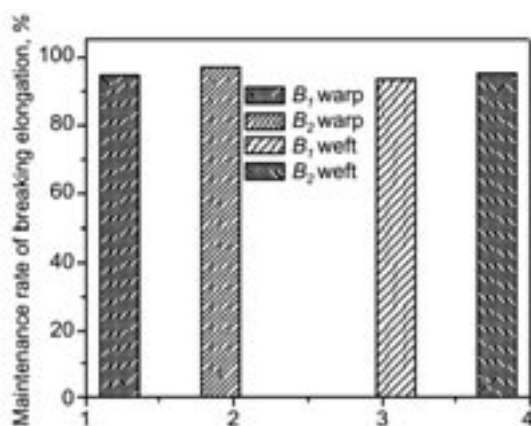


Fig. 8. The maintenance rate of the breaking elongation under 200°C treatment

interspaced, the quantity of light transmission is very low. The satin weave is long float and relaxed; so, more light can be transmitted. These reveal the fact that the fabrics transmittance largely depends on the fabrics surface. The lower the materials transmission rate is, the better the materials protective performance is. Thereby, we can choose the broken twill weave as a light protective material [12].

#### Effects of temperature on the fabric tensile properties

The effect of temperature on the fabric' tensile properties is shown in figures 7 and 8; thus, we can find the maintenance rate of the aramid fabric breaking strength shows a little decrease under 200°C, and the warp and the weft directions have little difference. The maintenance rate of the breaking strength for the Kevlar fabric is 88% and the breaking elongation is 94%. However, the blended fabric has higher such rates, whose maintenance rate of the breaking strength and elongation are 90% and 94%. The maintenance rate of

the breaking force is greater for the blended fabric than for the Kevlar fabric. The aramid fabrics have a great thermal stability. At the same time, we can improve the stability under high temperature, by choosing the blended fabric.

#### CONCLUSIONS

The following conclusions can be drawn from this study. Although the Kevlar 49 has high strength, low elongation and high rigidity, the strength loss rate is large in the weaving process. In order to improve the yarns utilization rate, we need to decrease the fiber damage in the weaving process.

The different weave patterns have different tensile, abrasion resistance, reflection and transmission performances. The fancy weave has the best tensile strength. The broken twill weave has a great transmission performance, yet, the fancy and satin weaves have great reflection performances. The Nomex/Kevlar blended fabric has a better reflection performance than the Kevlar fabric. The materials transmission rate is lower, yet, the materials protective performance is better. This indicates the broken twill weave blend fabric has better protective properties to temperature and light. The aramid fabrics show little breakage under 200°C temperature and a great thermal stability. Compared to pure fabrics, the blended fabrics have great thermal and light radiation stability. Therefore, we should choose a different fabric, according to the protective feature required.

#### ACKNOWLEDGEMENTS

We are grateful to the **Commission of Science, Technology and Industry for National Defense** for the financial support. The authors are also thankful to the members of **Textile Material and Technology Lab** for their help.

#### BIBLIOGRAPHY

- [1] Singleton, R. W., Kunkel R. H. *Factors influencing the evaluation of actinic degradation of fiber*. In: Textile Res. Journal, 1965, vol. 35, issue 3, p. 228
- [2] Day, M., Wiles, D. M. *Effect of light on the flammability of Nomex fabric*. In: Textile Res. Journal, 1974, vol. 44, issue 11, p. 888
- [3] Gozde, G., Burcu, A. *Moisture sorption and thermal characteristics of poly-aramid blend fabrics*. In: Journal of Applied Polymer Science, 2007, vol. 102, issue 1, p. 29
- [4] Iauk, W., Dias, T. *Knittability of high-modulus yarns*. In: Journal of Textile Institute, 1994, vol. 85, issue 2, p. 173
- [5] Jihan, S., Siddiqui, A. M. *Fracture strength of E-glass fiber strands using acoustic emission*. In: NDT & E International, 1997, vol. 30, issue 6, p. 383

- [6] Yao, J. W., Yu, W. D. *Tensile strength and its variation of pan-based carbon fibers. III. Weak-link analysis*. In: Journal of Applied Polymer Science, 2008, vol. 110, issue 10, p. 3 778
- [7] Liu, X. Y., Yu, W. D. *Evaluation of the tensile properties and the thermal stability of ultra-high molecular weight polyethylene fibers*. In: Journal of Applied Polymer Science, 2006, vol. 15, issue 16, p. 18
- [8] Liu, X. Y., Yu, W. D. *Evaluation of the thermal stability of high performance fibers by TGA*. In: Journal of Applied Polymer Science, 2006, vol. 99, issue 3, p. 937
- [9] Scelzo, W. A., Backer, S., Boyce, M. C. *Mechanistic role of yarn and fabric structure in determining tear resistance of woven cloth*. In: Textile Res. Journal, 1994, vol. 64, issue 5, p. 291
- [10] Cai, Z. X. *Fabric structure and design*. In: Beijing Textile Industry Press, 1990, p. 209
- [11] Hearle, J. W., Zhou, C. Y. *Tensile properties of twisted para-aramid fibers*. In: Textile Res. Journal, 1987, vol. 57, issue 1, p. 7
- [12] Cioară, L., Cioară, I., Toma, D. *Relația structură – proprietăți pentru țesături antistatice, destinate echipamentelor de protecție*. În: Industria Textilă, 2010, vol. 61, nr. 2, p. 81

#### Authors:

CAI GUANG MING

Textile materials and technology laboratory  
Donghua University, Shanghai  
201620 China  
e-mail: guangmingcai2006@163.com

YU WEIDONG

College of garment & art design  
Jiaxing University, Jiaxing  
Zhejiang 314001 China

## CRONICĂ



### A V-A CONFERINȚĂ ANUALĂ A PLATFORMEI TEHNOLOGICE EUROPENE PENTRU VIITORUL TEXTILELOR ȘI ÎMBRĂCĂMINTEI

În perioada 24–25 martie 2010, la Bruxelles, s-a desfășurat cea de-a V-a Conferință publică anuală a Platformei Tehnologice Europene pentru Viitorul Textilelor și al Îmbrăcăminte, cuprinzând 20 de clustere și programe naționale și regionale de inovare în domeniul textilelor din întreaga Uniune Europeană. La eveniment au participat peste 130 de reprezentanți ai industriei și mediului academic din Europa, dar și reprezentanți ai Comisiei Europene și ai presei internaționale de specialitate. Aceste inițiative, dintre care multe create în ultimii cinci ani, copiază și completează, la nivel național și regional, ceea ce însăși Platforma Tehnologică Europeană realizează la nivelul U.E.

Dezvoltarea unor rețele de centre C-D, coordonate la nivel național și racordate la rețele europene și internaționale de profil ridică profilul sectorului, ca industrie high-tech bazată pe cunoaștere, ce realizează produse cu o înaltă valoare adăugată și oferă locuri de muncă de un înalt nivel calitativ. Ele angajează autoritățile publice în direcția finanțării proiectelor de cercetare și transfer tehnologic realizate în colaborare/parteneriat, a trasării direcțiilor de dezvoltare tehnologică și realizării de studii prospective, a organizării de acțiuni de educare și instruire sau de acțiuni destinate cooperării internaționale. Locutori, reprezentanți ai Comisiei Europene, au prezentat câteva scheme de finanțare a proiectelor și programelor regionale de inovare, prin intermediul fondurilor structurale și regionale administrate de U.E. sau prin intermediul Programului Cadru 7 pentru Cercetare al U.E. Un alt program al U.E., schema ERA-Net, încurajează cumulul de fonduri regionale și naționale pentru cercetare publică, destinate proiectelor colaborative transfrontaliere de cercetare. Prin CrossTexNet, a fost lansat recent primul program de acest fel, dedicat cercetării textile. La proiect participă 17 agenții naționale și regionale de finanțare a cercetării din 11 state, printre care Franța, Italia, Germania și Spania. Programul a lansat primul apel pentru propuneri de proiecte în data de 30 aprilie 2010.

Având în vedere numărul mare de clustere de inovare prezentate în cadrul conferinței, Massimo Marchi, vicepreședinte al Consiliului Administrativ al Platformei Tehnologice, a afirmat: „*Consider că toate aceste inițiative demonstrează faptul că din ce în ce mai mulți oameni consideră colaborarea – dintre factorii publici și privați, dintre industrie, cercetare și autoritățile publice, dintre furnizorii și beneficiarii inovării – o cheie a succesului viitor. Lumea noastră devine mai complexă, piețele mai internaționalizate și mai versatile, produsele și serviciile mai sofisticate și interconectate, procesele și operațiunile mult mai tehnologizate. Succesul nu se mai bazează doar pe competențe exclusiv proprii, pe optimizarea proceselor interne sau pe iluzia unei piețe tradiționale predictibile*“.

În cuvântul de deschidere, Dr. Peter Pfneisl – președinte EURATEX, exprimându-și satisfacția legată de nivelul înalt al implicării autorității publice în diverse inițiative ale inovării textile, a reamintit că există o serie de domenii care trebuie optimizate. Pentru a avea mai mult succes în viitor, sunt necesare:

- un acces mai bun și o combinație mai abilă a tuturor surselor posibile de finanțare pentru creșterea numărului de acțiuni colaborative de inovare, în special în noile state membre, care până acum au fost slab reprezentate;
- o cooperare mai bună între inițiativele existente pe plan european, pentru un schimb util de informații și pentru a evita o copie inutilă a acestora;
- un management eficient al acestor structuri și o optimizare a utilizării resurselor financiare disponibile, astfel încât pentru fiecare euro, din banii publici cheltuiți, să se realizeze un beneficiu economic de peste un euro;
- o mai bună comunicare și promovare a inițiativelor la nivelul publicului larg, pentru a crea o industrie bazată pe cunoaștere, inovatoare și vizionară.

*Informații de presă. EURATEX, martie 2010*

# Modelling of the simultaneous wet spinning-grafting process of hemp fibres meant for medical textiles

AURELIA GRIGORIU  
CRISTINA RACU

RODICA MARIANA DIACONESCU  
ANA-MARIA GRIGORIU

## REZUMAT – ABSTRACT – INHALTSANGABE

### Modelarea procesului simultan de filare umedă-grefare a fibrelor de cânepă destinate textilelor medicale

Lucrarea prezintă modul în care monoclorotriazinil- $\beta$ -ciclodextrina poate fi grefată pe fibre liberiene, concomitent cu filarea umedă, în vederea obținerii unui material textil cu proprietăți funcționale noi, pentru aplicații medicale. În scopul găsirii valorilor optime ale parametrilor procesului, s-au efectuat încercări de prelucrare simultană, mecanică și chimică, la diferiți parametri de filare umedă-grefare și s-au folosit metodele matematice ale analizei dispersionale și ale regresiei.

Cuvinte-cheie: fibre, cânepă, filare umedă, grefare, modelare matematică, parametri

### Modelling of the simultaneous wet spinning-grafting process of hemp fibres meant for medical textiles

The present article studies the way in which monoclorotriazinil- $\beta$ -cyclodextrin can be grafted on bast fibres simultaneously with the wet spinning, in order to achieve a textile material with new functional properties, for medical applications. For determining the optimal values of the process parameters, several simultaneous mechanical and chemical processing trials have been achieved, at different wet spinning-grafting parameters and the mathematical methods of dispersion analysis and regression were applied.

Key-words: fibers, hemp, wet spinning, grafting, mathematical modelling, parameters

### Die Modellierung des simultanen Nassspinn-Pfropfprozesses der Hanffaser bestimmt für medizinische Textilien

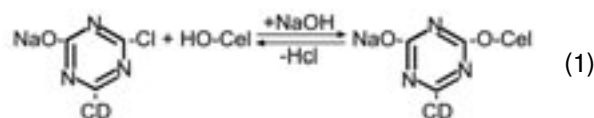
Die Arbeit umfasst die Art und Weise in der das Monochlorotriazinyl- $\beta$ -Cyclodextrin auf Bastfaser gepfropft werden kann, simultan mit dem Nassspinnen, im Sinne der Erhaltung eines Textilmaterials mit neuen funktionellen Eigenschaften für medizinische Anwendungen. Es wurden zum Zweck der Ermittlung der Optimalwerte der Prozessparameter Versuche für die simultane mechanische und chemische Prozessierung bei unterschiedlichen Nassspinn-Pfropfparameter durchgeführt und es wurden die mathematische Methoden der Dispersion-Analyse und der Regression angewendet.

Schlusswörter: Faser, Hanf, Nassspinnen, Pfropfen, mathematische Modellierung, Parameter

Due to the astonishing progress in the fields of the supramolecular chemistry, nanotechnology and polymer technology during the last years, a large number of drug delivery systems have been developed: cyclodextrins grafted on textiles, azo-crown ethers or fullerenes, ion exchange fibres, drug-loaded hollow fibres, textiles treated with nanoparticles and fibres containing bioactive compounds in their structure. Cyclodextrins have been successfully immobilized, by physical or chemical bonds, on the surface of fabrics [1, 2, 3]. When treating textiles with nanoparticles that contain an active compound (a drug for instance), nanoparticles are permanently fixed on the fabric through chemical bonds either by direct reaction between the particle and the textile, or by a linking molecule [4, 5]. Due to the specific molecular structure, with a hydrophobic interior and a hydrophilic exterior, cyclodextrins (CDs) are useful compounds for (hydrophobic) drugs inclusion [1, 4, 6]. The inclusion or the delivery of substances by the grafted CDs can be used for medical applications [5, 6, 7].

In the framework of a larger research, we have aimed at the elaboration of a conceptual model of a nanometrically finished textile material (made of flax or hemp fibres) for medical application, by grafting reactive compounds and obtaining cyclodextrins' inclusion compounds with bioactive properties. In the first stage we have analysed the way in which the reactive cyclodextrin monochlorotriazinyl- $\beta$ -cyclodextrin (MCT- $\beta$ -CD) can be grafted on bast fibres materials simultaneously with the wet spinning. These original elements are important for this field due to time and

labour savings, allowing the extension of the bast fibres' application in the medical sector by obtaining ecological products with new functional properties. The grafting of MCT- $\beta$ -CD on the cellulosic support takes place according to the reaction (1):



For the modelling of the wet spinning-grafting process, several trials of simultaneously mechanical and chemical processing have been made, with different wet spinning-grafting parameters (the concentration and the speed of the material in the impregnation stage) in order to establish the optimum parameters of the process.

During the wet spinning, in the drafting system of the spinning machine an individualization of the technical bast fibers and even of the elementary fibres has been realized, the obtaining of high fineness flax or hemp yarns being therefore possible.

In order to remove the non-cellulosic matters (pectins, waxes, lignin) that bond the elementary fibres, it is necessary their soaking. This is realized by the passage of the roving through a water tank and the adjustment of the drafting assembly's gauge at a smaller size than the average length of the technical bast fibres.

The yarns made of bast fibres have a very small breaking elongation, approximately 3%, and a high unevenness of the fineness, causing a great number of breaks during spinning. During the wet spinning, by passing the roving through the immersion tank, the substances

in the lamella that bond the elementary fibres become wet, jellyfy, behaving like a lubricant, therefore not only the technical fibres but also the elementary ones would slide one beside the other during drafting. By increasing the number of fibres in the cross section, the unevenness and the number of spinning breaks decrease [8, 9, 10].

This paper presents a modeling study based on experiments designed for the wet spinning-grafting process of hemp fibres. It was decided to use D-optimal design, as this is an effective method for obtaining maximum information with a minimum of experiments, and to determine which factors significantly influence the measured variables. The independent variables, the soaking time of the roving in the tank of the wet spinning machine –  $X_1$ , and the concentration of MCT- $\beta$ -CD –  $X_2$ , were considered and the tenacity and breaking elongation were chosen as response (dependent) variables. A composed central rotatable program for two independent variables was realized, tested and validated.

The resulting models were used for the optimization by the method simplex Nelder-Mead. The maximum values for the response function and the conditions in which these can be achieved were obtained, necessary data for the optimum process management.

## EXPERIMENTAL PART

Due to the great length of the bundle, the high sort hemp tow, which was used to obtain yarns before being introduced in the process, was cut at a length of approximately 80 cm, value determined by the constructive characteristics of the vertical hackling machine. The tow has undergone a manual precombing process, a combing with a vertical hackling machine and then it was recombed to straighten the ends of the tow bundle. Afterwards, the fibres were processed on a preparation technological flow characteristic to the spinning mills with combing technological process. To ensure a high quality, the sliver obtained with the sliver making machine was evened twice with a doubling machine. Four drafting frames followed by the roving frame were used, and the spinning was realized in wet state.

The modification of the time while the roving is soaked in the water tank of the wet spinning machine can be done in two ways: by changing the feeding speed or by the modification of the length of the path that the roving takes in the tank.

The modification of the feeding speed can be practically achieved on the machine by changing the belt pulleys, which are part of the first transmission after the electric motor of the spinning machine. By changing this transmission ratio, the drafting and the torsion are not modified, but the working parameters after the feeding creel and the water tank will not be identical, as the speed of the working devices will change at the same time with the feeding speed. Therefore, although the same draft will be kept, with a different delivery speed and a different spindle speed, one cannot assert that the processing of fibers strand after the water tank could be done in the same conditions. Therefore, in order to observe the way in which the soaking time of

the roving influences the characteristics of the yarns, the variant of modifying the path length through the water tank is better than the one in which the feeding speed was modified.

In order to render evident the influence of the chosen parameters, a greater interval of variation was chosen, that is a length of the path of the roving of 70 mm minimum and 770 mm maximum. The modification of the roving path length through the water tank was achieved by the guide pulleys within the tank and the liquor quantity introduced in the tank.

The physico-mechanical characteristics of the processed yarn spun in different conditions (different soaking times and different concentrations of MCT- $\beta$ -CD) were measured according to the standardized methodology. A Tinus Olsen H5KT electronic dynamometer according to the standard ISO 2062 and a electronic analytical balance were used. The mathematical methods of dispersion analysis and regression [11, 12] were applied in order to obtain the optimum values of the process parameters.

## RESULTS AND DISCUSSIONS

Firstly, we aimed at establishing a multiple, simultaneous correlation between:  $X_1$  – the soaking time of the roving in the tank of the wet spinning machine,  $X_2$  – the concentration of MCT- $\beta$ -CD and the resultant characteristic, respectively  $Y_1$  – the tenacity of the hemp yarn which has a medium linear density of 78 tex. The regression equation resulted after testing the correctness of coefficients and the adequacy of the mathematical model is the following:

$$Y_1 = 12.294 + 0.40576 X_1 + 1.06551 X_2 - 0.674007 X_1^2 - 0.541467 X_2^2 \quad (1)$$

For the model expressed by the equation (1), the linear and square components were successively analyzed. For the linear component of the equation (1), one can conclude that, between the two observed parameters, the concentration of MCT- $\beta$ -CD ( $X_2$ ) has a greater influence on the resultant characteristic, because the coefficient of the independent variable  $X_2$  is approximately 2.6 times higher than the one of variable  $X_1$ .

The signs of the coefficients of the linear component are positive for both parameters; taking into account that the resultant is the yarn tenacity, we have obviously aimed at maximizing this function, therefore the behaviour of the model for the simultaneous variation towards the limits of the experimental region of the two considered parameters,  $X_1$  and  $X_2$  (figure 1–4).

The value of the multiple correlation coefficient,  $R = 0.9727327$ , proves that there is a direct proportionality relation between  $X_1$  – the soaking time of the roving,  $X_2$  – the concentration of MCT- $\beta$ -CD and  $Y_1$  – the tenacity of the hemp yarn (the increase of  $X_1$  and  $X_2$  leads to the increase of  $Y_1$ ), the correlation being important ( $R$  very close to 1).

Analyzing the regression equation (1), it is noticeable that the coefficient of interaction corresponding to the term  $X_1X_2$  is missing, meaning that the effect of the simultaneous variation of the two parameters is not cumulative.

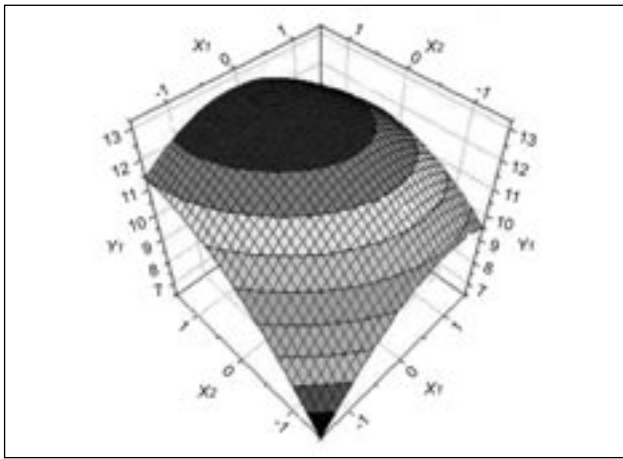


Fig. 1. The 3-D response surface for the resultant characteristic, the yarn tenacity

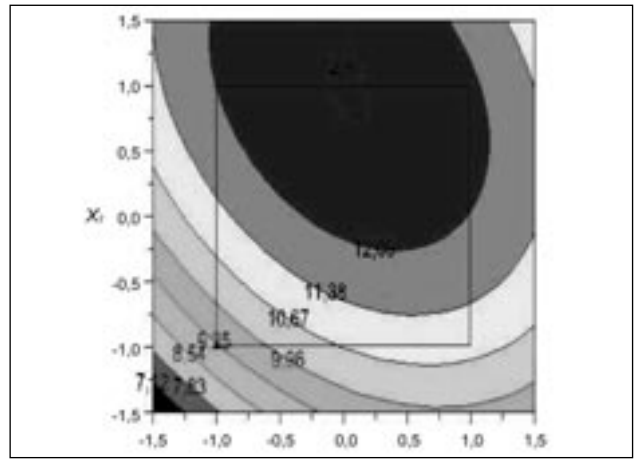


Fig. 2. Constant contour line of the yarn tenacity

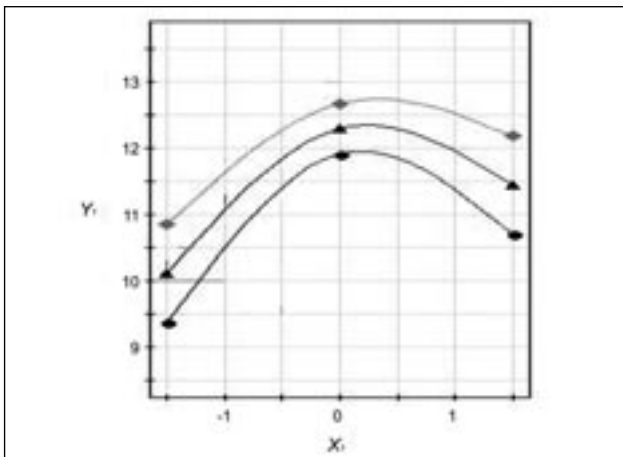


Fig. 3. Modification of the tenacity (independent variable  $Y_1$ ) depending on the soaking time of the roving (independent variable  $X_1$ ), for  $X_2 = X_{2c}$

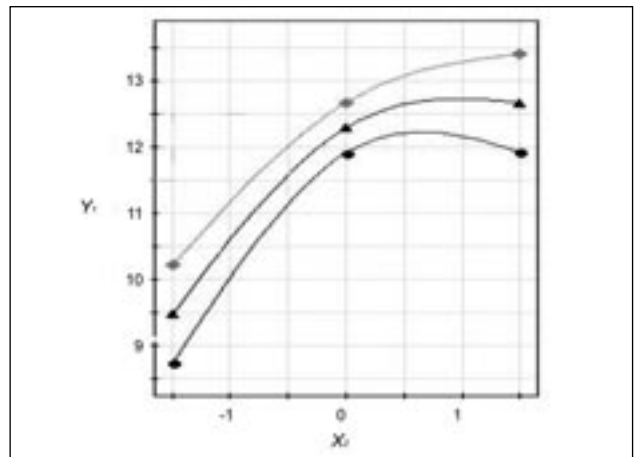


Fig. 4. Modification of the tenacity (independent variable  $Y_1$ ) depending on the concentration of MCT- $\beta$ -CD ( $X_2$ ), for  $X_1 = X_{1c}$

The following statements regarding the square component of the equation can be made: the presence of the square terms for both  $X_1$  and  $X_2$  has confirmed the existence of a well outlined surface, a rotation ellipsoid with a maximum point, corresponding to the previous claim of maximization; in this case there is also a difference between the absolute values of the square terms' coefficients,  $X_1^2$  having a coefficient with 25% bigger than the one corresponding to  $X_2^2$ ; the negative sign of these coefficients proves that the square term influences the objective function when decreasing, regardless of way in which the considered parameters change.

A maximum value of the tenacity of the yarn of 12.8193 cN/tex was obtained for a soaking time of 24.25 seconds and a concentration of 71.71 g/L MCT- $\beta$ -CD.

A second experiment aimed at establishing a multiple, simultaneous correlation between the soaking time of the roving in the tank of the wet spinning machine, the concentration of MCT- $\beta$ -CD and the resultant characteristic, the elongation of the hemp yarn (figure 5–8).

The regression equation resulted after testing the correctness of coefficients and the adequacy of the mathematical model is the following:

$$Y_2 = 3.0918 - 0.0853874 X_2 - 0.288304 X_1^2 + 0.349889 X_2^2 \quad (2)$$

For the model expressed by equation (2), a reasoning similar to the one used for the analysis of model (1). In this case, the analysis of the linear component of the equation has shown:

- between the two analyzed parameters, only the concentration of MCT- $\beta$ -CD –  $X_2$ , influences the resultant, the terms corresponding to the soaking time and to the variable  $X_1$  missing;
- the sign of the coefficient of the linear component for parameter  $X_2$  is negative, therefore the influence consists in the decreasing of the tenacity. The effect is not major due to the low value of the coefficient.

After the interpretation of the square component of model (2), aconstatat that have:

- the presence of square terms for both  $X_1$  and  $X_2$  confirmed the existence of a well outlined surface ("saddle" surface);
- is also a difference between the values of the coefficients of square terms,  $X_1^2$ , having a smaller coefficient than the one corresponding to  $X_2^2$ , and their signs are different; the negative sign of the coefficient for the variable  $X_1$  shows the square term influences the resultant when increasing, and the positive sign of the coefficient for variable  $X_2$  shows that the square term influences the resultant when increasing, regardless of the direction the considered parameter changes.

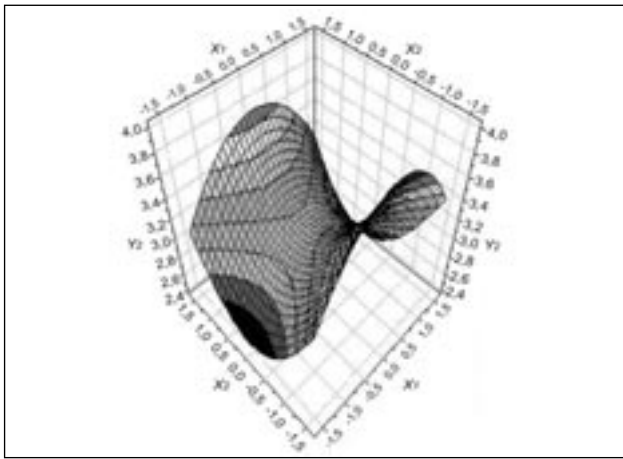


Fig. 5. The 3-D response surface of the resultant variable, for the yarn elongation

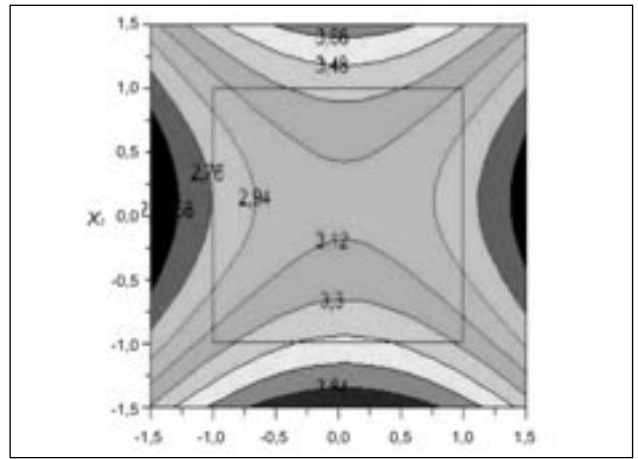


Fig. 6. Constant contour lines the yarn elongation

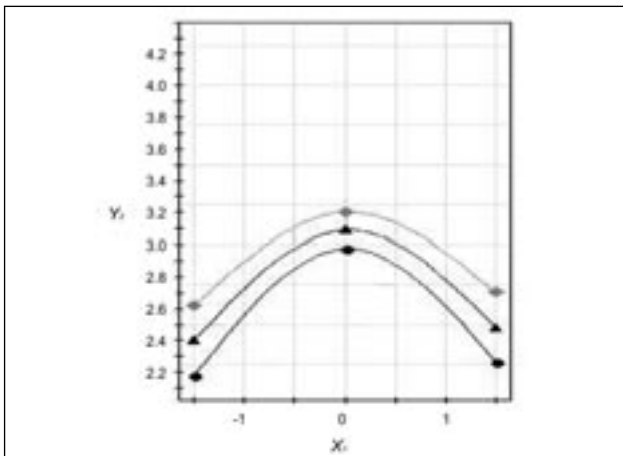


Fig. 7. Modification of the breaking yarn elongation (independent variable  $Y_2$ ) depending on the soaking time of the roving (independent variable  $X_1$ ), for  $X_2 = X_{2c}$

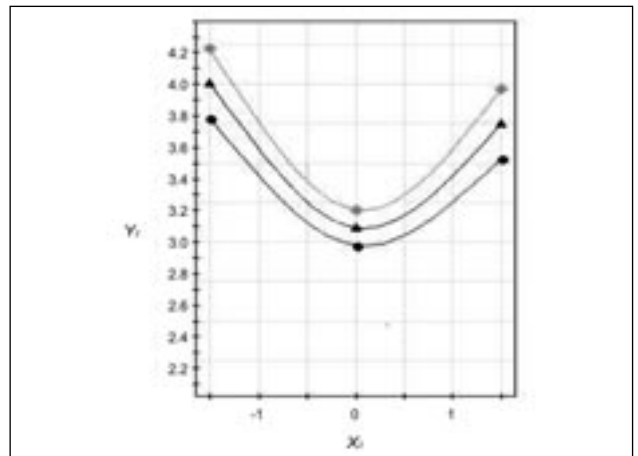


Fig. 8. Modification of the breaking yarn elongation (independent variable  $Y_2$ ) depending on the concentration of MCT- $\beta$ -CD ( $X_2$ ), for  $X_1 = X_{1c}$

The model expressed by the regression equation (2) has the interaction coefficient corresponding to the term  $X_1X_2$  null too, meaning the effect of simultaneous variation of the two parameters is not cumulative.

The influence of the two parameters,  $X_1$  – the soaking time of the roving and  $X_2$  – the concentration of MCT- $\beta$ -CD, on the elongation of the hemp yarn is rendered evident by the value of the coefficient of multiple correlation,  $R = 0.986446$ .

For the investigated experimental range, a maximum value of the yarn elongation of 4.0343% is obtained for a soaking time of the roving of 27.9 seconds and a concentration of MCT- $\beta$ -CD of 24.48 g/L.

## CONCLUSIONS

The experiments which have been performed aimed mainly at analysing the changes of mechanical characteristics of the yarn which has the average length density of 78 tex, and was spun from 100% hemp, depending the change of soaking time of the roving in the water tank of the wet spinning machine, and the MCT- $\beta$ -CD concentration in the tank.

A maximum value of 12.8193 cN/tex for the yarn tenacity may be obtained for a soaking time of 24.45 seconds and the MCT- $\beta$ -CD concentration of

71.71 g/L. As, from the technological point of view, the maximization of this parameter was aimed at, the value of the soaking time of the roving should be close to the centre of the experimental program and the value of the concentration of MCT- $\beta$ -CD should be close to the superior extremity of the considered experimental range.

A maximum value of 4.0343% for the yarn elongation may be obtained for a soaking time of the roving of 27.9 seconds and the MCT- $\beta$ -CD concentration of 24.48 g/L. This fact requires a value of the soaking time of the roving close to the centre of the experimental program and a value of the solution concentration close to the inferior limit of the considered range.

Taking into account that, between the two analysed mechanical characteristics, the tenacity and the yarn elongation, the latter is the one to be maximized at a higher extent than the former, which for a bast-type yarn has values high enough, a lower concentration of MCT- $\beta$ -CD, respectively 28.48 g/L, would be preferable. Simultaneous experiments performed with regard to the way in which the soaking time and concentration of MCT- $\beta$ -CD influence the grafting degree have proved that values of the concentration close to the centre of the experimental program, respectively 55 g/L MCT- $\beta$ -CD, are required.

Therefore, in order to obtain physico-mechanical characteristics adequate for a 100% hemp yarn and an optimum grafting degree for the ulterior inclusion operation to follow, it is necessary to establish for the simultaneous wet spinning-grafting process, a soaking time of 23.7 seconds and a solution concentration of 55 g/L MCT- $\beta$ -CD.

The reactive cyclodextrin, monochlorotriazinyl- $\beta$ -cyclo-

dextrin (MCT- $\beta$ -CD) can be grafted on bast fibres simultaneously with the wet spinning in order to obtain a nanometrically finished textile material for medical applications (after grafting, bioactive compounds will be included in the nanocavities of the reactive product). Therefore, the application fields for bast fibres may be extended to the medical sector by obtaining ecological products with new functional properties.

#### BIBLIOGRAPHY

- [1] Kistamah, N., Carr, C. M., Rosunee, S. *Surface chemical analysis of tencel and cotton treated with a monochlorotriazinyl (MCT)  $\beta$ -cyclodextrin derivative*. In: Journal Mater. Sci., 2006, vol. 41, p. 379
- [2] Ehen, Z., Giordano, F., Sztatisz, J., Jicsinszky, L., Novak, Cs. *Thermal characterization of natural and modified cyclodextrins using TG-MS combined technique*. In: Journal Therm. Anal. Cal., 2005, vol. 80, p. 419
- [3] Grechim, A. E., Buschmann, H. J., Schollmeyer, E. *Quantification of cyclodextrins fixed onto cellulose fibers*. In: Text. Res. Journal, 2007, vol. 77, issue 3, p. 161
- [4] Ten Breteler, M. R., Nierstrasz, V. A., Warmoeskerken, M. M. C. G. *Textile slow release systems with medical applications*. In: Autex Res. Journal, 2002, vol. 2, issue 4, p. 175
- [5] Shimizu, Y., Dohmyou, M., Yoshikawa, M., Takagishi, T. *Dyeing chitin/cellulose composite fibers with reactive dyes*. In: Text. Res. Journal, 2004, vol. 74, issue 1, p. 34
- [6] Szejtli, J. *Past, present and future of cyclodextrin research*. In: Pure Appl. Chem., 2004, vol. 76, issue 10, p. 1 824
- [7] Grigoriu, A.-M. *Cercetări în domeniul compușilor de incluziune ai ciclodextrinelor și al derivaților acestora, cu aplicații în industria textilă*. Teză de doctorat. Universitatea Tehnică Gheorghe Asachi, Iași, 2009
- [8] Cuzic-Zvonaru, C. *Contribuții la studiul și perfecționarea filării ude a firelor tip in*. Teză de doctorat. Universitatea Tehnică Gheorghe Asachi, Iași
- [9] Racu, C., Cuzic-Zvonaru, C., Preda, C. *Noi generații de fire filate ud din cânepă în amestec cu polipropilenă, pentru industria tricotajelor*. În: Industria Textilă, 1999, vol. 50, nr. 3, p. 149
- [10] Racu, C. *The influence of the wet spinning parameters upon the characteristics of yarns spun from hemp and wool blend*. Buletinul Institutului Politehnic din Iași, secția Textile-Pielărie, tomul LIV (LVIII), fasc. 3-4, 2008, p. 9
- [11] Zhang, H., Zhang, L. *Structural changes of hemp fibres modified with chitosan and BTCA*. În: Industria Textilă, 2010, vol. 61, nr. 2, p. 51
- [12] Mihail, R. *Introducere în strategia experimentării cu aplicații din tehnologia chimică*. Editura Științifică și Enciclopedică, București, 1976, p. 99
- [13] Taloi, D. *Optimizarea proceselor metalurgice*. Editura Didactică și Pedagogică, București, 1983, p. 76

#### Autori/Authors:

Prof. dr. ing./Prof. dr. eng. AURELIA GRIGORIU  
Șef de lucrări dr. ing./Chief of works dr. eng. CRISTINA RACU  
Asist. cerc. biochim. dr./Assist. biochim. researcher dr. ANA-MARIA GRIGORIU  
Universitatea Tehnică Gheorghe Asachi  
Facultatea de Textile-Pielărie și Management Industrial  
Bd. D. Mangeron nr. 53, 700050 Iași/  
Gheorghe Asachi Technical University  
Faculty of Leather-Textiles  
53 D. Mangeron Bvd., 700050 Iași  
e-mail: augrigor@tex.tuiasi.ro; crsracu@tex.tuiasi.ro;  
ana\_maria\_grigoriu@yahoo.co.uk

Conf. dr. ing./Conf. dr. eng. RODICA MARIANA DIACONESCU  
Universitatea Tehnică Gheorghe Asachi  
Facultatea de Inginerie Chimică și Protecția Mediului  
Bd. D. Mangeron nr. 71 A, 700050 Iași/  
Gheorghe Asachi Technical University  
Faculty of Chemical Engineering and Environment Protection  
71A D. Mangeron Bvd., 700050 Iași  
e-mail: rodicamdiaconescu@yahoo.com



# The effect of various production parameters on the physical properties of polypropylene meltblown nonwovens

DENIZ DURAN

SEHER PERINCEK

## REZUMAT – ABSTRACT – INHALTSANGABE

### Efectul diferiților parametri de producție asupra proprietăților fizice ale neșesutelor polipropilenice, filate din topitură

Filarea din topitură este un proces versatil și eficient, din punct de vedere al costurilor, de producere a materialelor neșesute din microfibră, direct din rășini termoplastice. Neșesutele filate din topitură, datorită microstructurii acestora, se caracterizează prin greutate redusă, suprafață mare, porozitate, moliciune și capacitate de absorbție. Diferitele tipuri de vâl neșesut filat din topitură pot fi utilizate în multe domenii, cum ar fi: filtrare, izolare, îmbrăcăminte, lavete, dar și în medicină. În lucrare, s-a studiat efectul diferiților parametri de producție asupra proprietăților fizice ale materialelor neșesute propilenice, filate din topitură.

Cuvinte-cheie: filare din topitură, neșesute, polipropilenă, microfibră, extrudare

### The effect of various production parameters on the physical properties of polypropylene meltblown nonwovens

Meltblowing is a versatile and cost effective process for producing microfiber nonwovens directly from thermoplastic resins. Due to their microstructure, meltblown nonwovens are characterized by lightweight, high surface area, porosity, softness and absorbency. Different types of meltblown nonwoven webs can be used in many application fields, such as: filtration, insulation, apparel, wipes and in medicine. In this paper, the effect of various production parameters on the physical properties of PP meltblown nonwovens was investigated.

Key-words: meltblowing, nonwovens, polypropylene, microfiber, extrusion

### Effekt der verschiedenen Produktionsparameter auf die physischen Eigenschaften der polypropylenischen Spinnvliesstoffe

Das Spinnvliesverfahren ist ein vielseitiges und effizientes Prozess, aus dem Sichtpunkt der Kosten, was die Produktion der Vliesstoffe aus Mikrofaser direkt aus thermoplastischen Harze, anbelangt. Die Spinnvliesstoffe charakterisieren sich dank ihrer Mikrostruktur durch geringes Gewicht, grosse Oberfläche, Porosität, Weichheit und Absorptionskapazität. Die verschiedenen Typen von Spinnvliesstoffe können in vielfachen Bereichen angewendet werden, wie z.B.: Spinnen, Dichten, Bekleidung, Tücher aber auch im medizinischen Bereich. In der Arbeit wurde der Effekt der verschiedenen Produktionsparameter auf die physischen Eigenschaften der polypropylenischen Vliesstoffe, untersucht.

Schlusswörter: Vliesspinnen, Vliesstoffe, Polypropylen, Mikrofaser, Extrudieren

The demand for nonwovens is increasing throughout the world day-by-day. Nonwoven materials are processed differently from the conventional textile fabrics, web forming and web consolidation techniques being used. They are produced on the basis of individual fibers, by using different processes, such as meltblowing, spun-bonding etc.

Meltblowing is a kind of microfiber nonwoven production process, which uses thermoplastic polymers to attenuate the melt filaments, with the aid of high-velocity air. Polypropylene (PP) is the polymer most widely used for this process, since it is relatively inexpensive and versatile enough to produce a wide range of products. Other polymers, such as polyethylene (PE), poly(ethylene terephthalate) (PET), poly(butylene terephthalate) (PBT), polystyrene, polyurethane (PUR), and polyamide (PA), can also be used to produce meltblown webs [2, 6].

Meltblowing has become an important industrial technique in nonwovens, because of its ability to produce materials suitable for filtration media, thermal insulators, battery separators, oil absorbents, medical area, miscellaneous applications, apparel area, wipes, and many laminate applications [6–9]. The basic meltblowing process is illustrated in figure 1. The polymer is melted in an extruder, pumped through die-holes and then the melt enters high-speed, hot air streams. Web structure begins to develop when fiber entanglement first occurs, yet network structure becomes fixed only when fibers contact the collector and their motion ceases [3].

The meltblown process generally consists of five major components: extruder, metering pump, die assembly,

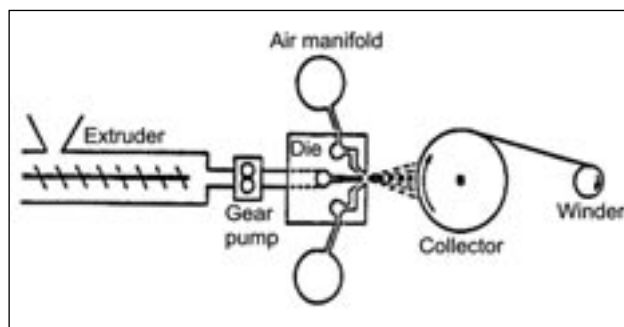


Fig. 1. Schematic view of the meltblowing process

web formation, and winding. In the extruder, the polymer resin is heated and melted until appropriate temperature and viscosity are reached. The molten polymer is then fed to the metering pump to ensure uniform polymer feed to the die assembly. The microfibers are formed when the molten polymer exiting the die hits a hot, high velocity air. The microfibers are collected on a moving screen or drum, where the self-bonded web is formed [6].

The extruder is the component responsible for melting the polymer by heat and feeding it to the metering pump. The extruder is composed of three different zones, namely: zone 1 (the feed zone), zone 2 (the transition zone), zone 3 (the metering zone). The polymer mixture, preheated in the feed zone, is then pushed to the transition zone where it is compressed and homogenized, before being pushed to the metering zone. The polymer pressure is the greatest in the metering zone, thus the polymer mixture being forwarded to the metering pump.

Table 1

MAIN PRODUCTION SETTINGS AND THEIR VALUES USED IN EXPERIMENTS	
Production setting	Value
Extruder zone 1 temperature, °F	300
Extruder zone 2 temperature, °F	350
Extruder zone 3 temperature, °F	400
Die temperature, °F	390
Air temperature, °F	400
Die hole diameter, inches	0.09

The metering pump is a component important in maintaining the pressure required for the extruder to uniformly and consistently deliver the molten polymer to the die assembly.

The die assembly is directly responsible for the web formation, web quality and uniformity and therefore it is the most important element of the meltblowing system. The feed distribution plates are responsible for keeping the plate heated at a consistent and proper temperature, in order to maintain even the polymer flow and to obtain some stable polymer properties. Polymer-distribution is also influenced by the shape of the feed-distribution. The polymer is fed to the die holes from the feed distribution plate. The die nosepiece is largely responsible for the fiber diameter, quality and uniformity. The air manifold is responsible for supplying the high velocity air, which is an important factor in the polymer drawing and attenuation to then form the micro-fibers. The air manifold is located on the sides of the die nosepiece and supplies hot, high-velocity air into the polymer, within which the die tip is placed. The web formation begins at this point [6].

The complexity of the process comes when the number of variables and the interaction between the process variables are taken into consideration. In this paper, the influence of die-to-collector distance (DCD), collector drum speed, collector vacuum, die air pressure, extruder pressure, and extruder speed was investigated on web structure properties such as – thickness, basis weight, air permeability, tensile properties, surface friction and fiber diameter.

## EXPERIMENTAL PART

In this study, the effect of some production parameters on the physical properties of polypropylene (PP) meltblown nonwovens was investigated.

As raw material, PP was used with a 1100 melt flow rate (MFR), 0.75 g/cm<sup>3</sup> density, and a 335°F melting point.

The main production settings namely: extruder temperature, die temperature, air temperature (air fed to the spinneret for fibers spinning), and die hole diameter are given in table 1.

The production parameters of the PP meltblown nonwovens investigated are as follows:

- die-to-collector distance (DCD);
- collector drum speed;
- collector vacuum;
- die air pressure;
- extruder pressure;
- extruder speed.

The sample codes and production parameters of the PP meltblown nonwovens investigated in this study can be seen in table 2.

The samples produced were characterized for thickness, basis weight, tensile properties, air permeability, surface friction and fiber diameter.

*Thickness* was tested by using SDL Thickness Gauge, according to TS 7128 EN ISO 5084 standard, with 20 cm<sup>2</sup> measurement area under 200 g weight.

*Tensile properties* were tested according to TS EN ISO 13934-1 standard, by using Zwick Z010 Universal tensile strength with 200 mm measurement distance and 100 mm/minute measurement speed.

*Air-permeability* test was performed by using FX 3300 Air permeability test device, according to TS 391 EN ISO 9237 standard, with 20 cm<sup>2</sup> measurement area and 100 Pa air pressure.

*Surface friction* properties of the samples were tested in the Frictorq Test Device developed by University of Minho Mechatronics Laboratory.

*Fiber-diameter* was measured by using Leica DM EP light microscope with 400 zoom.

## RESULTS AND DISCUSSIONS

In this study, quantitative experimental measurements were performed as well as some statistical analysis on the influence of die air pressure, extruder speed, die-to-collector distance (DCD), extruder pressure, collector drum speed, and collector vacuum over the thickness, basis weight, air permeability, surface friction, fiber

Table 2

SAMPLE CODES AND PRODUCTION PARAMETERS OF THE PP NONWOVENS						
Sample code	DCD, cm	Collector drum speed, ft/min.	Collector vacuum, %	Die air pressure, psi	Extruder pressure, psi	Extruder speed, %
Sample 1	30	25	20	11	712	50
Sample 2	30	25	40	11	712	50
Sample 3	30	25	40	9	714	50
Sample 4	30	25	40	13	712	50
Sample 5	40	25	20	11	680	50
Sample 6	40	25	20	11	814	50
Sample 7	40	60	60	13	695	50
Sample 8	50	60	60	13	683	50
Sample 9	60	25	20	11	599	80
Sample 10	60	25	20	11	636	60
Sample 11	60	25	60	13	698	50
Sample 12	60	25	40	13	693	50
Sample 13	60	60	60	13	694	50

ANOVA TEST RESULTS				
Parameters	Properties	Mean square	F	Sig.
Die air pressure	Thickness	3.481E-02	136.217	0.000
	Basis weight	2.111	9.500	0.014
	Air permeability	660341.778	44684.782	0.000
	Surface friction	4.944E-03	82.260	0.000
	Fiber diameter	2.982	76.851	0.000
	Tensile strength	2.159	0.104	0.903
Extruder speed	Thickness	7.000E-04	136.217	0.835
	Basis weight	86.333	0.186	0.000
	Air permeability	150.111	155.400	0.000
	Surface friction	1.104E-03	46.586	0.028
	Fiber diameter	1.960	6.937	0.000
	Tensile strength	54.645	41.880	0.046
DCD	Thickness	2.841E-02	255.700	0.000
	Basis weight	0.111	0.250	0.787
	Air permeability	89920.778	2423.015	0.000
	Surface friction	1.928E-04	14.038	0.05
	Fiber diameter	1.929	4.390	0.067
	Tensile strength	0.465	3.341	0.106
Extruder pressure	Thickness	3.668E-02	62.283	0.000
	Basis weight	45.444	102.250	0.000
	Air permeability	3700.111	174.351	0.000
	Surface friction	2.868E-03	26.287	0.001
	Fiber diameter	1.792	17.163	0.003
	Tensile strength	22.558	0.766	0.506

diameter, and the tensile properties of polypropylene meltblown non-woven webs.

When the significance and  $F$  values were taken into consideration, it could be clearly seen that:

*The fiber diameter* is influenced most substantially by die air pressure, moderately by extruder speed, slightly by extruder pressure and insignificantly by DCD (table 3). Die air pressure had a significant influence on mean fiber diameter in webs. This was thought to be associated with the influence of die air pressure on the polymer viscosity, through the entire die-collector space. As die air-pressure was increased, mean fiber diameter decreased.

Although DCD does not influence the fiber diameter, *the thickness property* of the polypropylene non-woven webs was significantly associated with the DCD ( $F$  value = 255.7). The effect of the extruder speed onto the thickness can be regarded as ineffective.

*The basis weight* of non-woven webs is designated by the extruder speed. The extruder pressure seemed to have been the second important parameter. DCD with 0.787 significance value (higher than 0.05) does not have a statistically important effect in terms of the basis weight.

When the results were investigated in terms of *the air permeability property*, the statistical importance of the die air pressure with 44 684  $F$  value differs from the others. The DCD, extruder pressure, and extruder speed ensue from the die pressure.

Nearly the same situation occurs when the investigated parameter is *the surface friction*: the effective parameter is the die air pressure and then extruder pressure, DCD, and extruder speed.

On the other hand, *tensile strength property* of webs was affected by just the extruder speed. In order to clearly see the effects of these parameters onto the

web properties, Duncan post-hoc test has been performed.

### Thickness

The thickness property of meltblown nonwovens is known to be effected mostly by drum speed, collector vacuum and DCD. Thickness increases with the decrease in the collector drum speed.

When the collector drum speed decreased from 60 ft/min. to 25 ft/min., the web thickness value increased from 0.15 mm to 0.53 mm (samples 11 and 13). The decrease in the collector vacuum is known to cause a thickness increase in the meltblown nonwovens.

When figure 2 is observed, it can be seen that sample 1, with a 0.57 mm thickness value, shows a relatively higher thickness result compared to sample 2, with a 0.42 mm thickness value. A similar result is achieved when samples 11 and 12 are taken into consideration. This is thought to be caused by the low collector vacuum values in their production. DCD has an impact on thickness as well. Thickness increases with the DCD increase. This trend is visible when the results of samples 8 and 13 are taken into consideration. The DCD was increased from 50 cm to 60 cm during the production of sample 13. Consequently, the thickness value increased from 0.13 mm to 0.15 mm.

On the other hand, Duncan post-hoc test results showed that the increase at the die air pressure caused the increase in thickness. For example, the thickness value increased from 0.38 mm to 0.58 mm by the increase of the die air pressure from 9 psi to 13 psi. A similar trend was obtained when the independent parameter was the extruder pressure. When table 2 and figure 2 are observed, it can be seen that sample 6 thickness-value increased from 0.42 mm to 0.64 mm just by decreasing the extruder pressure from 814 psi to 680 psi.

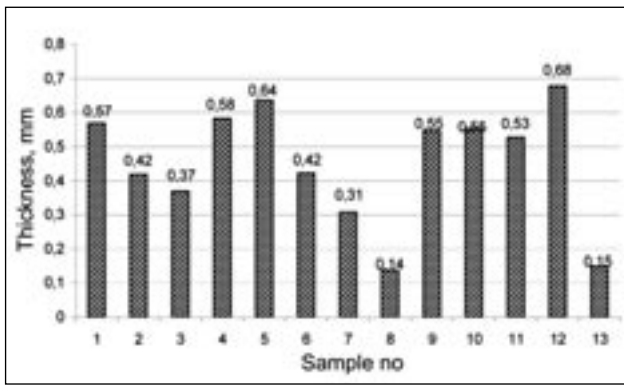


Fig. 2. Effect of production parameters onto the samples thickness

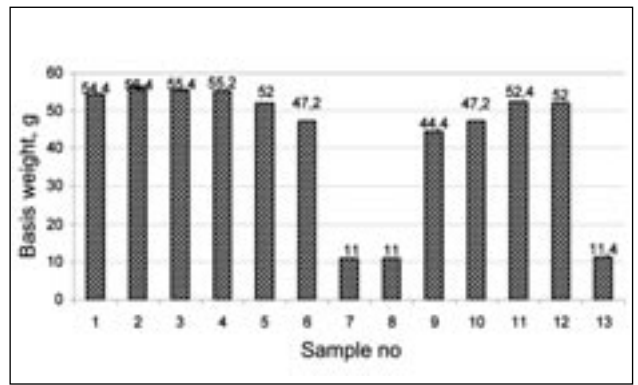


Fig. 3. Effect of production parameters onto the samples basis-weight

Table 4

DUNCAN POST-HOC TEST RESULTS RELATED TO THE EFFECT OF DIE AIR PRESSURE AND EXTRUDER PRESSURE ON THE SAMPLES THICKNESS							
Die air pressure				Extruder pressure			
	Subset				Subset		
Sample no:	1	2	3	Sample no:	1	2	3
5(3)	0.38			21(6)	0.42		
6(2)		0.42		3(1)		0.57	
7(4)			0.58	19(5)			0.64
Sig.	1.000	1.000	1.000	Sig.	1.000	1.000	1.000
Alpha = 0.05				Alpha = 0.05			

### Basis weight

Basis weight is an important physical property of nonwoven materials. The basis weight of meltblown nonwovens is mostly affected by the collector drum speed. The higher the collector drum speed is, the lower the basis weight becomes. Figure 3 shows that sample 13, which was produced with the highest collector drum speed (60 ft/min.) used in this study, exhibited lower basis weight results than sample 11, which was produced with the lowest collector drum speed (25 ft/min.).

When ANOVA test results in table 4 are observed, it can be seen that extruder speed, extruder pressure and die air pressure are the other important factors affecting the basis weight of meltblown nonwovens. Table 5 shows that the decrease in the extruder speed causes the increase of the basis weight. The basis weight value of the web reached nearly 55, if the extruder speed was decreased from 80% to 50%. So, it is clearly seen from the ANOVA test results that the effect of the extruder speed onto the basis weight is more important than the effect of the die air pressure. Duncan test results supported this idea as well. The variation at the

extruder speed caused significant differences between the basis-weights of the samples. Yet, the change in the die air pressure caused nearly the same basis weight (56 g/m<sup>2</sup>).

### Air permeability

Air permeability is related to the structural characteristics of nonwovens. In figure 4, it can be seen that samples 13, 8 and 7 have shown the highest air permeability results, whereas the lowest results were obtained for samples 4, 11, 2, 12 and 1. The reason of this result can be that the decrease in fiber diameter, thickness and basis weight causes the increase in the air permeability of nonwovens. When figures 2, 3 and 4 are observed, it can be clearly seen that this trend was valid: samples 13, 8 and 7 exhibited low test results in terms of basis weight, thickness and fiber diameter. There is a different situation for samples 4, 11 and 12, showing low air permeability results in spite of their low fiber diameter results, but this was thought to be caused by high thickness and basis weight results. Low air-permeability results of samples 1 and 2 can be explained by the low fiber diameter.

ANOVA test results have shown that die air pressure, extruder speed, DCD, and extruder pressure have a significant effect on air permeability. Among these parameters, die air pressure appears to be the major factor considering the value  $F = 44\ 684$ . When observed the Duncan post-hoc test results in table 6, it can be seen these have supported the ANOVA test results. When the die air pressure was set to 9, 11 and 13 psi during the production, the air permeability property of the nonwoven samples was 133, 108, 93 g/m<sup>2</sup>/l. The extruder speed was increased from 50% to 80% during the production and, as a result, samples with a higher air permeability property were achieved. ANOVA

Table 5

DUNCAN POST-HOC TEST RESULTS RELATED TO THE EFFECT OF DIE AIR PRESSURE AND EXTRUDER SPEED ON THE SAMPLES BASIS-WEIGHT						
Die air pressure			Extruder pressure			
	Subset			Subset		
Sample no:	1	2	Sample no:	1	2	3
7(4)	55.00		18(9)	44.33		
5(3)	55.67		17(10)		47.00	
6(2)		56.67	3(1)			54.67
Sig.	0.134	1.000	Sig.	1.000	1.000	1.000
Alpha = 0.05			Alpha = 0.05			

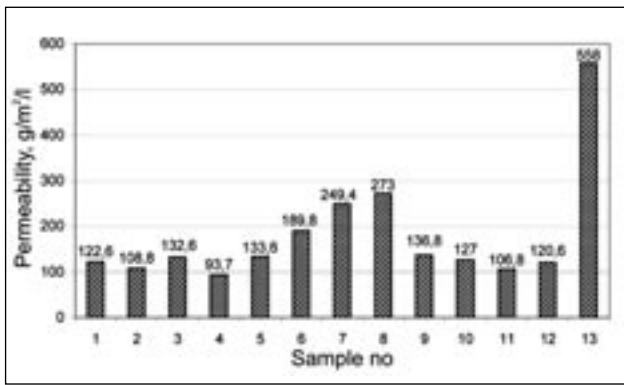


Fig. 4. Effect of production parameters onto the samples air-permeability

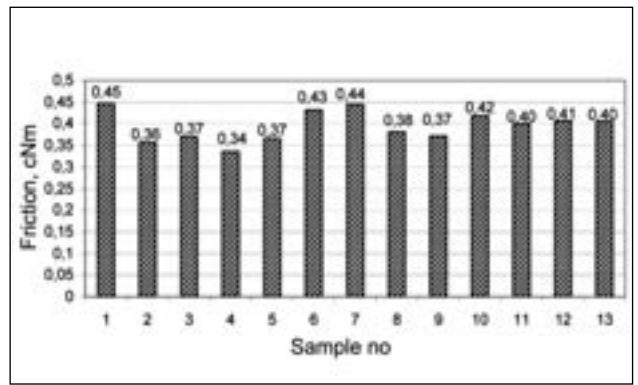


Fig. 5. Effect of production parameters onto the samples surface-friction

Table 6

DUNCAN POST-HOC TEST RESULTS RELATED TO THE EFFECT OF DIE AIR PRESSURE, EXTRUDER SPEED AND DCD ON THE SAMPLES AIR-PERMEABILITY											
Die air pressure				Extruder speed				DCD			
	Subset				Subset				Subset		
Sample no:	1	2	3	Sample no:	1	2	3	Sample no:	1	2	3
6(2)	108.33			3(1)	123.0			14(7)	250.33		
5(3)		133.0		1(10)		126.67		13(8)		271.0	
7(4)			93.3	18(9)			136.67	12(13)			560.0
Sig.	1.000	1.000	1.000	Sig.	1.000	1.000	1.000	Sig.	1.000	1.000	1.000
Alpha = 0.05				Alpha = 0.05				Alpha = 0.05			

Table 7

DUNCAN POST-HOC TEST RESULTS RELATED TO THE EFFECT OF DIE AIR PRESSURE, EXTRUDER SPEED AND EXTRUDER PRESSURE ON THE SAMPLES SURFACE-FRICTION											
Die air pressure				Extruder speed				Extruder pressure			
	Subset				Subset				Subset		
Sample no:	1	2	3	Sample no:	1	2	3	Sample no:	1	2	3
5(3)	0.34			3(1)	0.41			21(6)	0.38		
6(2)		0.37		17(10)	0.43	0.43		3(1)		0.41	
7(4)			0.42	18(9)			0.45	19(5)			0.44
Sig.	1.000	1.000	1.000	Sig.	0.078	0.164		Sig.	1.000	1.000	1.000
Alpha = 0.05				Alpha = 0.05				Alpha = 0.05			

test results in table 3 showed that DCD was the second important parameter in terms of air permeability. When the distance between collector and die increased, voluminous samples were obtained. Therefore, the air permeability properties of samples were the highest.

### Surface friction

Surface friction is an important factor, affecting the end use properties of the nonwoven materials. When ANOVA test results in table 3 are observed, it can be seen that die air pressure, extruder pressure, DCD and extruder speed have a significant effect on the surface friction of meltblown nonwovens. Surface becomes smoother and friction decreases with the decrease in DCD. As it can be seen in figure 5, sample 8 that was produced with a lower DCD value (50 cm) than sample 13 (60 cm) showed lower surface resistance results. Another important factor influencing the surface friction of meltblown nonwovens is the collector vacuum. Surface friction decreases with the increase in collector vacuum. As figure 5 shows, sample 1 had a higher surface friction value due to its low collector vacuum value, as compared to other samples, even though it was produced with a low DCD. This result proved the

significance that the impact of collector vacuum parameter has on the surface friction of meltblown nonwovens.

When table 7 and figure 6 are observed, it can be seen that, among samples 2, 3 and 4 produced with the same DCD, collector vacuum, collector drum speed and extruder speed values, sample 3 had a higher surface friction value, because of the higher die air

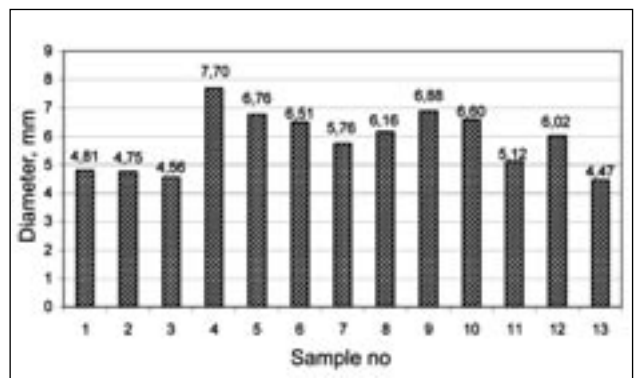


Fig. 6. Effect of production parameters onto the samples fiber-diameter

DUNCAN POST-HOC TEST RESULTS RELATED TO THE EFFECT OF DIE AIR PRESSURE, EXTRUDER SPEED AND EXTRUDER PRESSURE ON THE SAMPLES FIBER DIAMETER									
Die air pressure			Extruder speed			Extruder pressure			
	Subset			Subset			Subset		
Sample no:	1	2	3	Sample no:	1	2	Sample no:	1	2
6(2)	6.38			17(10)	6.55		21(6)	6.74	
5(3)		7.01		18(9)	6.92		19(5)	6.77	
7(4)			8.34	3(1)		8.10	3(1)		8.10
Sig.	1.000	1.000	1.000	Sig.	0.083	1.000	Sig.	0.913	1.000
Alpha = 0.05			Alpha = 0.05			Alpha = 0.05			

Table 9

DUNCAN POST-HOC TEST RESULTS RELATED TO THE EFFECT OF THE EXTRUDER SPEED ON THE SAMPLES TENSILE-STRENGTH		
	Subset	
Sample no:	1	2
17(10)	15.88	
18(9)	16.87	
3(1)		23.72
Sig.	0.715	1.000
Alpha = 0.05		

pressure compared to other samples. This result was supported by the Duncan post-hoc test results. Meanwhile, as table 7 shows, the increase at the extruder speed and decrease at the extruder pressure caused samples with higher surface friction values.

#### Fiber diameter

The fiber diameter has a significant effect not only on the physical characteristics of nonwovens, but it also affects their end-use properties. The fiber diameter was found to be 4–7 mm for the meltblown nonwovens tested in our study, which gives them their unique microstructure, porosity and high surface area.

In the meltblowing process, fiber diameter is known to be affected by die air pressure, extruder pressure and extruder speed. This is also shown by ANOVA and Duncan post-hoc test results in tables 3 and 8. Among samples 2, 3 and 4, which were produced with the same extruder pressure, extruder speed and DCD values, sample 4 had higher fiber diameter results because of the highest die air pressure. A higher extruder speed causes higher fiber diameter values on the resulting meltblown web. The fiber diameter value of sample 9 is higher, compared to samples 1 and 10, which were produced with the same extruder pressure, DCD and die air pressure. This could be caused by higher extruder speed. The difference between the effect of samples 9 and 10 extruder speeds seems to be statistically insignificant, considering the Duncan post-hoc test results in table 8. When samples 6, 5 and 1 produced with the same die air pressure, extruder speed and DCD were compared, it was observed that samples 5 and 6 exhibit higher fiber diameter results, compared to sample 1, and the extruder pressure effect on the fiber diameters of samples 5 and 6 were statistically insignificant. Table 9 also shows that the increase at the die air pressure causes the increase in the fiber diameter.

#### Tensile properties

When figure 7 is observed, it can be clearly seen that samples 7, 8 and 13 show lower tensile strength and

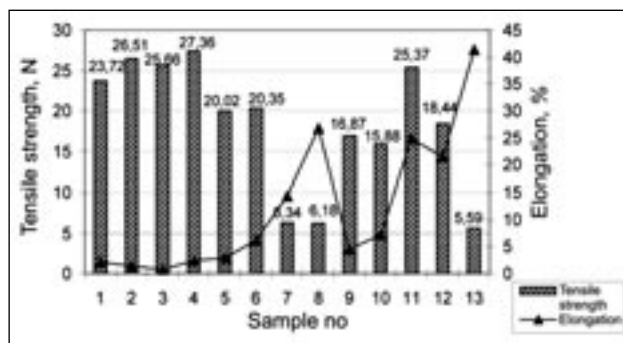


Fig. 7. Effect of production parameters onto the samples tensile-properties

higher elongation results, compared to other samples. Considering the results, it can be stated that, for the meltblown nonwovens in our study, the tensile strength increased and elongation decreased with the increase in the basis weight.

Statistical results obtained from the ANOVA test have shown that extruder speed had a significant effect on the tensile strength of the samples. Duncan post-hoc test showed that the decrease in the extruder speed supplied the samples a higher tensile strength property. When samples 7, 8 and 13 were taken into consideration, the effect of the DCD can be observed onto the elongation property of the nonwoven webs. The DCD increase from 40 cm to 60 cm caused the increase in elongation, but no significant change at the tensile strength value.

#### CONCLUSIONS

In this study, the effect of some production parameters – die-to-collector distance (DCD), collector drum speed, collector vacuum, die air pressure, extruder pressure and extruder speed – were investigated on the physical properties of the PP meltblown nonwovens. The physical properties tested were thickness, basis weight, air permeability, surface friction, fiber diameter and the tensile properties.

Results have shown that thickness was influenced mostly by DCD and collector drum speed. Thickness increased with the decrease in drum speed and the increase in DCD. It was observed that extruder speed, extruder pressure, die pressure and collector drum speed were the important factors affecting the basis weight. Basis weight decreased with the increase in collector drum speed. Fiber diameter was found to be affected by – die pressure, extruder pressure and extruder speed. Results of the tensile test have shown that the tensile strength of the nonwovens had a parallel

trend with their basis weight. It can be said that the tensile strength increased and elongation decreased with the increase in the basis weight. Air permeability test-results have shown that the decrease in – fiber diameter, thickness and basis weight – caused an increase in the air permeability of the meltblown nonwovens. The surface friction of the nonwovens tested decreased with the DCD decrease and the collector vacuum increase.

Meltblown nonwovens are a relatively new class of nonwoven materials, which integrate into new application areas, to replace conventional textile materials and gain more importance day-by-day. Due to their unique microstructure, porosity, absorbency, light-weight and high surface area, the microfiber meltblown nonwovens become promising materials for various application areas.

#### BIBLIOGRAPHY

- [1] Wei, Q., Li, Q., Wang, X., Huang, F., Gao, W. *Dynamic water adsorption behavior of plasma-treated polypropylene nonwovens*. In: Polymer Testing, 2006, vol. 25, p. 717
- [2] Zhang, D., Sun, C., Beard, J., Brown, H., Carson, I., Charles, H. *Development and characterization of poly(trimethylene terephthalate)-based bicomponent meltblown nonwovens*. In: Journal of Applied Polymer Science, 2002, vol. 83, p. 1 280
- [3] Bresee, R. R., Qureshi, U. A. *Influence of processing conditions on meltblown web structure. Part 1 – DCD*. INJ Spring, 2004, p. 49
- [4] Bresee, R. R., Qureshi, U. A. *Influence of processing conditions on meltblown web structure. Part IV – Fiber Diameter*. In: Journal of Engineered Fibers and Fabrics, 2006, vol. 1, issue 1, p. 32
- [5] Gahan, R., Zguris, G. C. *A review of the meltblowing process*, p. 145
- [6] Dutton, Kathryn C. *Overview and analysis of the meltblowing process and parameters*. In: Journal of Textile and Apparel, Technology and Management (JTATM), 2008, vol. 6, issue 1
- [7] Zamfir, M., Fărimă, D., Ciocoiu, M., Ene, A. *Nonwovens based external end-uses hygiene and medical products*. În: Industria Textilă, 2009, vol. 60, nr. 6, p. 320
- [8] Crețu, C. V., Cojocaru, C., Preda, C., Macoveanu, M. *Materiale textile neșesute termocalandrate, din polipropilenă, utilizate pentru decontaminarea apelor poluate cu produse petroliere*. În: Industria Textilă, 2008, vol. 59, issue 6, p. 320
- [9] Moore, G. *The potential of recycled plastics as feedstock for the production of meltblown nonwoven webs*. Tappi Journal, TAPPI 1990 Nonwovens Conference, May 1990, p. 93

#### Authors:

DENIZ DURAN  
SEHER PERINCEK

Ege University  
Emel Akýn Vocational Training School  
Bornova, 35100 Izmir, Turkey  
e-mail: deniz.duran@ege.edu.tr



În cadrul editurii Certex a apărut cartea "Industria de textile și confecții din România".

Cartea prezintă informații utile tuturor producătorilor și comercianților de produse textile și confecții.

Editura  
**Certex**

Str. Lucrețiu Pătrășcanu nr. 16  
Sector 3, 030508 București, România  
Tel: (00402)1-340.49.28; 340.42.00  
Fax: (00402)1-340.55.15  
E-mail: certex@ns.certex.ro